In the saliva-VLP binding assay, we examined the possibility that NoV and SaV VLPs may bind to saliva samples. Briefly, 100 µl of serially diluted saliva samples dissolved in carbonate/bicarbonate buffer (50 mmol/L, pH 9.6) were added to wells and incubated at 37 °C overnight. The wells were washed 3–6 times with 300 µl of phosphate-buffered saline containing 0.05% Tween 20 (PBS-T) and washed again after each of the following steps. The wells were blocked with 200 µl of PBS containing 5% skim milk (SM/PBS) for 1 h at room temperature. The purified VLPs, dissolved in 1% SM/PBS-T (final 1 µg/mL), were added (100 µl) to the wells and incubated for 1 h at 37 °C. Next, 100 µl of rabbit anti-rSaV or NoV VLP antiserum (1:2000) in 1% SM/PBS-T was added, and incubated for 1 h at 37 °C. Horseradish peroxidase (HRP)-conjugated anti-rabbit IgG (100 µl; Zymed Laboratories Inc., San Francisco, CA, USA) in 1% SM/PBS-T was then added and incubated for 1 h at 37 °C. One hundred microliter of O-phenylenediamine (Sigma, St. Louis, MO, USA) was added as substrate, and incubated at room temperature for 30 min, at which point 50 µl of 4N H_2SO_4 was added to stop the reaction, and the optical density (OD) at 492 nm was measured. The wells incubated with carbonate/bicarbonate buffer instead of serially diluted saliva samples were used as plate blank (Fig. 1). The Hawaii VLPs have been reported to show no binding to HBGAs [5]; under the present experimental conditions, Hawaii VLPs also showed no binding activity (OD values less than 0.01) at all to HBGAs in saliva. The VLPs of the NoV 104 strain, which resembles Camberwell virus (AF145896) and is classified into GII/4, showed strong binding activity to the diluted saliva at all dilutions of all HBGA samples (OD values greater than 2.7), while SaV Mc114 VLPs showed little binding activity at all dilutions of all samples (OD less than 0.09), as did SaV NK24 VLPs (OD values less than 0.24). These results indicate that the SaV Mc114 and NK24 VLPs have no binding activity with saliva antigens.

In the carbohydrate-VLP binding assay, we examined the possibility that NoV and SaV VLPs may bind to different synthetic carbohydrates, such as H-1 (trisaccharides), A (trisaccharides), B (trisaccharides), Le^a (trisaccharides) and Le^b (tetrasaccharides). Briefly, multivalent carbohydrate-biotin reagents conjugated to polyacrylamide (CHO-PAA-biotin; GlycoTech, Rockville, MD, USA) were resuspended in 0.3 M sodium phosphate buffer at 1 mg/ml, diluted to 20 µg/ml in Tris-buffered saline, and serially diluted twofold, after which 100 µl was added per well to streptavidin-precoated plates (Thermo Labsystems, Basingstoke, United Kingdom) and incubated for 2 h at 37 °C. The wells were washed 3–6 times with PBS-T and were washed again after each of the following steps. The plates were blocked with 300 µl of 5% SM/PBS overnight at 4 °C. The VLPs (1 µg/ml in 100 µl of 5% SM/PBS) were added to each well and incubated for 4 h at 37 °C. Next, 100 µl of rabbit anti-rNoV VLPs antiserum (1:2000 in 5% SM/PBS) was added and incubated for 2 h at 37 °C. One hundred microliter of HRP-conjugated anti-rabbit IgG in 5% SM/PBS was then added and incubated for 1 h at 37 °C. The plates were processed as described above. The wells incubated with Tris-buffered saline and 5% SM/PBS instead of serially diluted synthetic carbohydrates and VLPs were used as plate blank.

The NoV 104 VLPs were found to show strong binding activity to three of five synthetic carbohydrates: A, B and Le^b (Fig. 2B, C and E). Although 104 VLPs showed strong binding activity to the saliva samples containing relatively high amounts of H antigen (Fig. 1A) and Le^a antigen (Fig. 1D), they showed only moderate binding activity to H synthetic carbohydrates and no binding activity to Le^a synthetic carbohydrates (Fig. 2A and D). Differences in the reactivity between saliva samples and synthetic carbohydrates may be due to differences between synthetic products and the authentic antigens found in vivo, which are thought to be present on mucin or mucin-like molecules [7]. Therefore, we included two additional NoV VLPs, the 124 and 258 VLPs, as positive controls for the H and Le^a synthetic carbohydrates (Fig. 2A and D), respectively, which showed strong binding activity to the H-high and Le^a-high saliva samples (data not shown). The 124 strain is genetically close to the GI/1 prototype Norwalk virus (NV/68; M87661), and the binding properties of recombinant NV/68

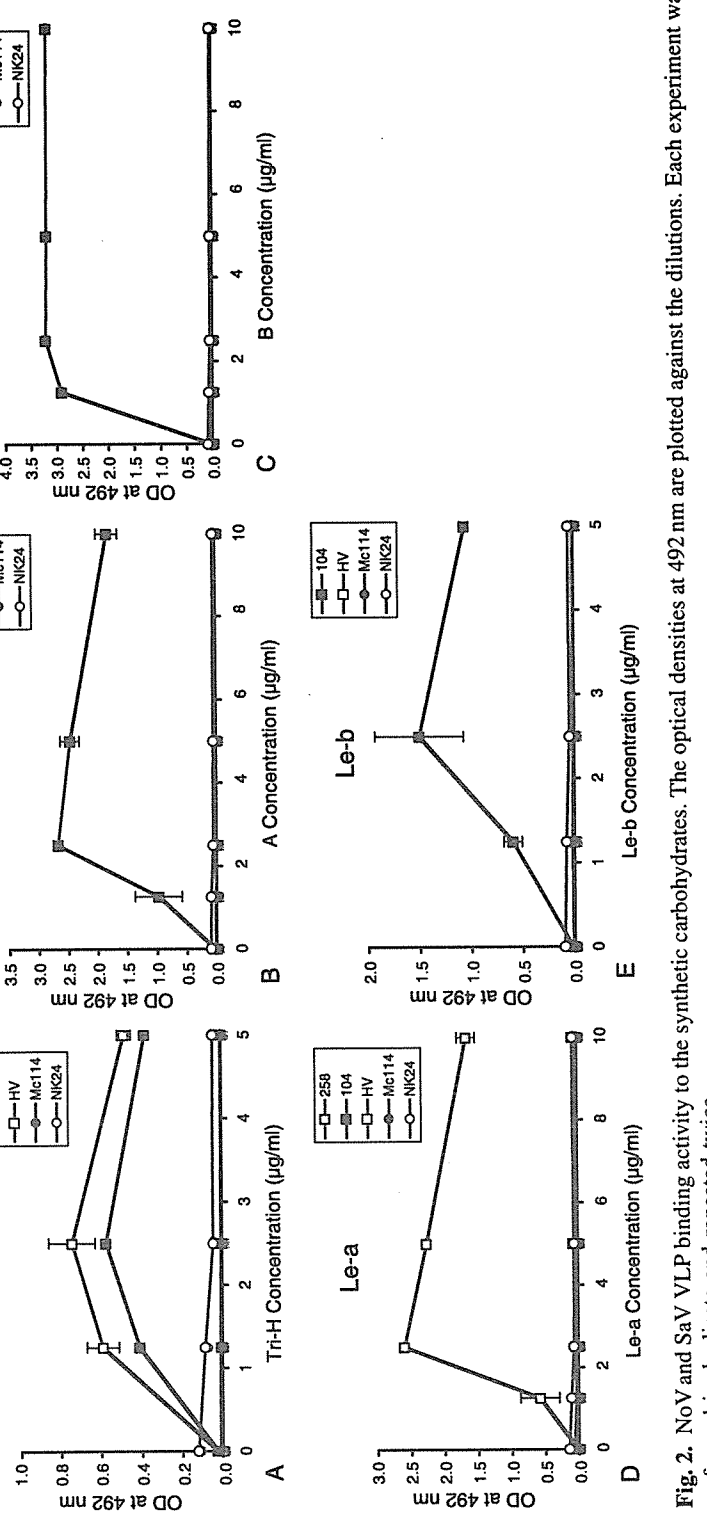

Fig. 2. NoV and SaV VLP binding activity to the synthetic carbohydrates. The optical densities at 492 nm are plotted against the dilutions. Each experiment was performed in duplicate and repeated twice

to H antigen have been well characterized [5, 13]. The 124 strain showed 99% amino acid identity with NV/68 in the P2 domain. There are known to be two amino acid differences at residues 370 and 376 which are not related to HBGA binding [14]. The 258 strain resembles Southampton virus (L07418) and is classified into GI/2. The NoV Hawaii VLPs showed no binding activity to any of these synthetic carbohydrates (Fig. 2). The SaV Mc114 and NK24 VLPs also showed no binding activity to any of the synthetic carbohydrates (Fig. 2).

A number studies have found that different NoV strains exhibit different binding patterns to HBGAs [5–7]. In the present study, we found that NoV GII/4 104 VLPs showed binding activity to HBGAs, while SaV GI and GV VLPs showed no such binding activity. Human SaVs are becoming an increasingly important cause of gastroenteritis worldwide [3, 4, 10]. Further studies are needed to examine the possibility that other human SaV genogroups have binding activity.

Acknowledgements

This work was supported in part by a grant for Research on Emerging and Re-emerging Infectious Diseases, Research on Food Safety from the Ministry of Health, Labor and Welfare of Japan, and by a grant for Research on Health Science Focusing on Drug Innovation from The Japan Health Science Foundation.

References

1. Farkas T, Zhong WM, Jing Y, Huang PW, Espinosa SM, Martinez N, Morrow AL, Ruiz-Palacios GM, Pickering LK, Jiang X (2004) Genetic diversity among sapoviruses. Arch Virol 149: 1309–1323
2. Hansman GS, Natori K, Oka T, Ogawa S, Tanaka K, Nagata N, Ushijima H, Takeda N, Katayama K (2005) Cross-reactivity among sapovirus recombinant capsid proteins. Arch Virol 150: 21–36
3. Hansman GS, Takeda N, Oka T, Oseto M, Hedlund KO, Katayama K (2005) Intergenogroup recombination in sapoviruses. Emerg Infect Dis 11: 1916–1920
4. Hansman GS, Takeda N, Katayama K, Tu ET, McIver CJ, Rawlinson WD, White PA (2006) Genetic diversity of Sapovirus in children, Australia. Emerg Infect Dis 12: 141–143
5. Harrington PR, Lindesmith L, Yount B, Moe CL, Baric RS (2002) Binding of Norwalk virus-like particles to ABH histo-blood group antigens is blocked by antisera from infected human volunteers or experimentally vaccinated mice. J Virol 76: 12335–12343
6. Huang P, Farkas T, Marionneau S, Zhong W, Ruvoen-Clouet N, Morrow AL, Altaye M, Pickering LK, Newburg DS, LePendu J, Jiang X (2003) Noroviruses bind to human ABO, Lewis, and secretor histo-blood group antigens: identification of 4 distinct strain-specific patterns. J Infect Dis 188: 19–31
7. Huang P, Farkas T, Zhong W, Tan M, Thornton S, Morrow AL, Jiang X (2005) Norovirus and histo-blood group antigens: demonstration of a wide spectrum of strain specificities and classification of two major binding groups among multiple binding patterns. J Virol 79: 6714–6722
8. Hutson AM, Atmar RL, Graham DY, Estes MK (2002) Norwalk virus infection and disease is associated with ABO histo-blood group type. J Infect Dis 185: 1335–1337
9. Jiang X, Wang M, Graham DY, Estes MK (1992) Expression, self-assembly, and antigenicity of the Norwalk virus capsid protein. J Virol 66: 6527–6532
10. Johansson PJ, Bergentoft K, Larsson PA, Magnusson G, Widell A, Thorhagen M, Hedlund KO (2005) A nosocomial sapovirus-associated outbreak of gastroenteritis in adults. Scand J Infect Dis 37: 200–204
11. Kageyama T, Shinohara M, Uchida K, Fukushi S, Hoshino FB, Kojima S, Takai R, Oka T, Takeda N, Katayama K (2004) Coexistence of multiple genotypes, including newly identified genotypes, in outbreaks of gastroenteritis due to Norovirus in Japan. J Clin Microbiol 42: 2988–2995
12. Lindesmith L, Moe C, Marionneau S, Ruvoen N, Jiang X, Lindblad L, Stewart P, LePendu J, Baric R (2003) Human susceptibility and resistance to Norwalk virus infection. Nat Med 9: 548–553
13. Marionneau S, Ruvoen N, Le Moullac-Vaidye B, Clement M, Cailleau-Thomas A, Ruiz-Palacois G, Huang P, Jiang X, Le Pendu J (2002) Norwalk virus binds to histo-blood group antigens present on gastroduodenal epithelial cells of secretor individuals. Gastroenterology 122: 1967–1977
14. Tan M, Huang P, Meller J, Zhong W, Farkas T, Jiang X (2003) Mutations within the P2 domain of norovirus capsid affect binding to human histo-blood group antigens: evidence for a binding pocket. J Virol 77: 12562–12571

JOURNAL OF VIROLOGY, Jan. 2007, p. 309–318
0022-538X/07/$08.00+0 doi:10.1128/JVI.01411-06

Vol. 81, No. 1

Regulation of CXCL-8 (Interleukin-8) Induction by Double-Stranded RNA Signaling Pathways during Hepatitis C Virus Infection[▽]

Jessica Wagoner,[1] Michael Austin,[1] Jamison Green,[1] Tadaatsu Imaizumi,[4] Antonella Casola,[5] Allan Brasier,[5] Khalid S. A. Khabar,[6] Takaji Wakita,[7] Michael Gale, Jr.,[8] and Stephen J. Polyak[1,2,3]*

Departments of Laboratory Medicine,[1] Microbiology,[2] and Pathobiology,[3] University of Washington, Seattle, Washington; Hirosaki University School of Medicine, Hirosaki, Japan[4]; Departments of Pediatrics and Medicine, University of Texas Medical Branch, Galveston, Texas[5]; Program in BioMolecular Research, King Faisal Specialist Hospital and Research Center, Riyadh, Saudi Arabia[6]; Department of Virology II, National Institute of Infectious Diseases, Tokyo, Japan[7]; and Department of Microbiology, University of Texas Southwestern Medical Center, Dallas, Texas[8]

Received 5 July 2006/Accepted 5 October 2006

Hepatitis C virus (HCV) infection induces the α-chemokine interleukin-8 (CXCL-8), which is regulated at the levels of transcription and mRNA stability. In the current study, CXCL-8 regulation by double-stranded (ds)RNA pathways was analyzed in the context of HCV infection. A constitutively active mutant of the retinoic acid-inducible gene I (RIG-I), RIG-N, activated CXCL-8 transcription. Promoter mutagenesis experiments indicated that NF-κB and interferon (IFN)-stimulated response element (ISRE) binding sites were required for the RIG-N induction of CXCL-8 transcription. IFN-β promoter stimulator 1 (IPS-1) expression also activated CXCL-8 transcription, and mutations of the ISRE and NF-κB binding sites reduced and abrogated CXCL-8 transcription, respectively. In the presence of wild-type RIG-I, transfection of JFH-1 RNA or JFH-1 virus infection of Huh7.5.1 cells activated the CXCL-8 promoter. Expression of IFN regulatory factor 3 (IRF-3) stimulated transcription from both full-length and ISRE-driven CXCL-8 promoters. Chromatin immunoprecipitation assays demonstrated that IRF-3 and NF-κB bound directly to the CXCL-8 promoter in response to virus infection and dsRNA transfection. RIG-N stabilized CXCL-8 mRNA via the AU-rich element in the 3′ untranslated region of CXCL-8 mRNA, leading to an increase in its half-life following tumor necrosis factor alpha induction. The data indicate that HCV infection triggers dsRNA signaling pathways that induce CXCL-8 via transcriptional activation and mRNA stabilization and define a regulatory link between innate antiviral and inflammatory cellular responses to virus infection.

Hepatitis C virus (HCV) infects an estimated 3% or 170 million of the world's population and causes an estimated 476,000 deaths per year due to complications of end-stage liver disease (56, 62). In the United States, about 1.8% of the general population or 4 million persons are infected. Of those acutely infected with HCV, approximately 85% develop chronic infection, and about 70% of these patients develop histological evidence of chronic liver disease. Moreover, viremia is not cleared in about 50% of infected patients treated with pegylated interferon (IFN)-ribavirin therapy, the current standard of care. Compounding this issue are the predictions that in the next 20 years, HCV-related complications, including hepatic decompensation, hepatocellular carcinoma, and liver-related deaths, will increase by 106%, 81%, and 180%, respectively (12). Thus, chronic hepatitis C is a serious global medical problem necessitating effective treatment. Given the propensity of HCV for chronic infection, association with severe liver disease, and difficulty of treatment, many studies are focused on HCV-host interactions that contribute to HCV persistence and pathogenesis.

The inflammatory response to virus infection involves the regulated induction of cytokines and chemokines. The response is initiated within the infected cell by pathogen-associated molecular pattern (PAMP) recognition but soon thereafter affects neighboring cells and tissues due to the paracrine effects of cytokine and chemokine release. Cytokine and chemokine release occurs rapidly in response to virus infection, and its chief objectives are to recruit inflammatory leukocytes, limit virus replication and spread, and induce adaptive immunity. However, prolonged expression of chemokines in the context of chronic viral infections may be detrimental to the host. For example, patients with chronic hepatitis C have elevations in serum levels of α-chemokine interleukin-8 (CXCL-8), and patients who are nonresponsive to IFN therapy have high pretreatment levels of CXCL-8 (39, 51). When expressed in cell culture, the HCV NS5A protein induces CXCL-8, which is associated with the inhibition of the antiviral effects of IFN (4, 16, 50).

CXCL-8 is a 71-amino-acid chemokine belonging to the CXC family and is produced by many cell types, including monocytes, epithelial cells, fibroblasts, and hepatocytes (42). CXCL-8 elicits many effects, including neutrophil, T-lymphocyte and basophil chemotaxis and degranulation, oxidative burst, and lysosomal-enzyme release (42). CXCL-8 has been shown to be an important mediator of the inflammatory responses to many viruses and bacteria. For example, CXCL-8 is induced in response to the expression of the HCV NS5A protein (3, 4, 16, 50) and HCV replication (19). Moreover,

* Corresponding author. Mailing address: University of Washington, Virology 359690, 325 9th Avenue, Seattle, WA 98104-2499. Phone: (206) 341-5224. Fax: (206) 341-5203. E-mail: polyak@u.washington.edu.

▽ Published ahead of print on 11 October 2006.

CXCL-8 inhibits the antiviral actions of IFN-α (29), and recent studies indicate that CXCL-8 protein levels are associated with HCV replication (30).

CXCL-8 is induced by a variety of stimuli, including those from CXCL-1, tumor necrosis factor alpha (TNF-α), phorbol esters, lipopolysaccharide, and virus infection (42). The induction of CXCL-8 involves both the transcriptional activation of the CXCL-8 promoter and the stabilization of CXCL-8 mRNA (61). CXCL-8 mRNA stabilization involves the binding of regulatory proteins to AU-rich elements (AREs) in the 3′ untranslated region (3′UTR) of the mRNA (1, 6, 9, 53). The CXCL-8 promoter contains binding sites for NF-κB, NF-interleukin 6 (IL-6), AP-1 protein, and an IFN-stimulated response element (ISRE)-like element, which has been shown to bind proteins belonging to the IFN regulatory factor (IRF) family (8, 65). The mechanisms of CXCL-8 gene induction have been investigated using different stimuli and cell types, and deletion and mutational analyses of the promoter indicate that CXCL-8 is activated in a cell-type- and stimulus-specific manner (43, 45). It has previously been shown that HCV NS5A-induced transcriptional activation of the CXCL-8 promoter requires intact NF-κB and AP-1 binding sites (4, 50). However, the role of upstream regulatory elements, such as the ISRE site, is not known.

IRF proteins play pivotal roles in innate antiviral responses and bind to DNA sequences containing ISREs (2, 36). IRFs are activated by virus infection when viral PAMPs, such as double-stranded (ds)RNA, are sensed by Toll-like receptor 3 (TLR3) or by cytoplasmic dsRNA sensors such as the retinoic acid-inducible gene I (RIG-I) (66). IPS-1 (also known as the MAVS, Cardif, or VISA protein) (21) is an adaptor protein for RIG-I signaling (34). RNA binding to RIG-I and interaction with IPS-1 or TLR3 activate IRF-3 and NF-κB. IRF-3 and NF-κB translocate to the nucleus, interact with other transcription factors, and bind to their cognate promoter elements to induce gene expression, which classically includes IFN-α and IFN-β genes.

IRFs and NF-κB also regulate transcription of chemokine genes. For instance, IRF-1 is involved in the respiratory syncytial virus (RSV) and *Helicobacter pylori* induction of CXCL-8 by binding to one of several ISRE-like elements in the CXCL-8 promoter (8, 65). Similarly, IRF-3 induces the chemokine RANTES by binding to ISREs in the RANTES promoter (32). Moreover, NF-κB is the principal transcription factor responsible for CXCL-8 induction (42). Thus, the regulation of chemokines by NF-κB and especially by IRFs may represent a functional link between innate antiviral and inflammatory responses. In the current report, we examined the induction of CXCL-8 by dsRNA-triggered innate antiviral pathways in the context of HCV infection in vitro.

MATERIALS AND METHODS

Cells and viruses. Human hepatoma Huh7 cells and HEK293 cells were grown in Huh7 medium which contained Dulbecco's minimum essential medium, 10% fetal bovine serum, 1× penicillin, streptomycin, amphotericin B (Fungizone) (except for HEK cells), 10 mM L-glutamine, and 1× nonessential amino acids (all reagents were from Invitrogen, Carlsbad, CA). Huh7 cells were obtained from Apath, LLC. Huh7.5.1 cells were obtained from Francis Chisari (68) and cultured in Huh7 medium. All cell lines were checked for mycoplasma by using a MycoAlert assay (Cambrex Bio Science, Rockland, ME) and found to be mycoplasma-free.

JFH-1 viral stock preparation, cell infection, and titration were performed exactly as described previously (59, 68).

Plasmids. BB7 replicon plasmid DNA was obtained from Apath, LLC. Generation of JFH-1 RNA and transfection of cells were performed as described previously (59). Various luciferase reporter genes under the control of different forms of CXCL-8 were also used and were obtained from Naofumi Mukaida (44) or generated as described previously (8) (see Fig. 1). Plasmid pQ150 expresses green fluorescent protein (GFP) under the control of the constitutive EF-1α promoter and was provided by Jeffery Vieira. Cytomegalovirus IRF-3 (CMV-IRF-3) (33) was obtained from John Hiscott. Wild-type RIG (RIG-WT), constitutively active (RIG-N), and dominant negative (RIG-C) plasmids were generated as previously described (14, 66).

Transfection. The day prior to transfection, 3×10^4 cells were plated in black, clear-bottomed, 96-well tissue culture plates. Endotoxin-free plasmid DNA was purified (Endofree kit; QIAGEN, Valencia, CA) and introduced into cells with Lipofectamine 2000 according to the manufacturer's recommendations (Invitrogen). For reporter gene studies, unless otherwise indicated, 100 ng of the luciferase gene under the control of the promoter construct of interest was transfected into cells in triplicate or quadruplicate. When expression plasmids were included in the transfection, 50 ng of each was added. Eighteen hours later, stimuli such as recombinant human TNF-α (rhTNF-α) (15 ng/ml; Pierce Biotechnology, Rockford, IL) or virus infection (Sendai virus at a multiplicity of infection [MOI] of 100 hemagglutinin units, or JFH-1 virus at an MOI of 0.01 focus-forming unit) were added to cells. In the case of poly(I) · poly(C) [poly(I:C)] (0.2 μg/well) or JFH-1 RNA (0.25 μg/well), cells were retransfected using Lipofectamine 2000 or transmessenger RNA (QIAGEN) reagents. Six h [for poly(I:C)] or 24 h later (for JFH-1 RNA), luciferase activity was measured on cell lysates using a Britelite assay system (Perkin Elmer, Boston, MA). Before protein harvest, cells were visualized under a fluorescent microscope, and the transfection efficiency was determined by comparing the proportion of GFP-positive cells to the total cell number, as described previously (30, 40, 47). The results, in relative light units, shown in Fig. 2, 3, and 4 are corrected for transfection efficiency.

Western blot analysis. Protein lysates were quantitated (BCA Protein Assay; Pierce), and equal amounts of total protein (10 to 20 μg) were separated on 4 to 20% sodium dodecyl sulfate-polyacrylamide electrophoresis (SDS-PAGE) gels. IRF-3 and Stat2 were detected using polyclonal antiserum (Santa Cruz Biotechnology). HCV proteins were detected using random, deidentified HCV-infected patient serum, as described previously (49). Prior to use, infected serum was inactivated by adding Triton X-100 to a final concentration of 1%. NS5A protein was also detected using a polyclonal antibody to NS5A (Chiron, Emeryville, CA). RIG proteins were detected using a polyclonal antibody (25).

RNA quantitation. CXCL-8 mRNA was quantitated by real-time reverse transcriptase (RT)-PCR, as recently described (19). Dilutions of precisely quantitated CXCL-8 cDNA in the PCMGSNEO plasmid (64) (kindly provided by Naofumi Mukaida), ranging from 0 to 10^7 copies per tube, were run in triplicate to generate a standard curve, which served as a reference to calculate the CXCL-8 copy number based on the cycle threshold. RNA copy numbers were normalized to 10 ng of total cellular RNA.

Chromatin immunoprecipitation assays. Chromatin immunoprecipitation (ChIP) assays were performed according to the manufacturer's specifications (Upstate USA, Charlottesville, VA). Briefly, 2×10^6 cells were plated on 10-cm dishes and then treated with various inducers, including TNF-α, poly(I:C) or encephalomyocarditis virus infection, for various times. Transcription factors were cross-linked to DNA by adding formaldehyde directly to culture medium to a final concentration of 1% and incubated for 10 min at 37°C. Cells were washed and scraped into phosphate-buffered saline containing 1 mM phenylmethylsulfonyl fluoride (PMSF), 1 μg/ml aprotinin, and 1 μg/ml pepstatin A. Cells were pelleted and resuspended in SDS lysis buffer (Upstate), and DNA was sheared into lengths of 200 to 1,000 base pairs by sonication at 50 V and 30% amplitude for a total of eight times for 5 seconds each on ice. Lysates were cleared by centrifugation for 10 min at 13,000 rpm at 4°C. Supernatants were diluted ninefold in ChIP dilution buffer (Upstate) and precleared with protein A agarose-salmon sperm DNA (50% slurry; Upstate) for 30 min at 4°C with agitation. One to two microliters of IRF-3 antibody (polyclonal, from Michael David, or monoclonal, from Pharmingen) was added to the precleared supernatants and incubated overnight with rotation at 4°C, followed by the addition of protein A agarose-salmon sperm DNA. ChIP samples were washed, DNA protein complexes eluted, cross-links reversed, and DNA extracted. CXCL-8 and IFN-B promoter-specific PCRs were performed using primer sets CXCL-8F (AAGAA AACTTTCGTCATACTCCG), CXCL-8R (TGGCTTTTTATATCATCACCC TAC), IFN-BF (CCTCACAGTTTGTAAATCTTTTTCCC), and IFN-BR (AC

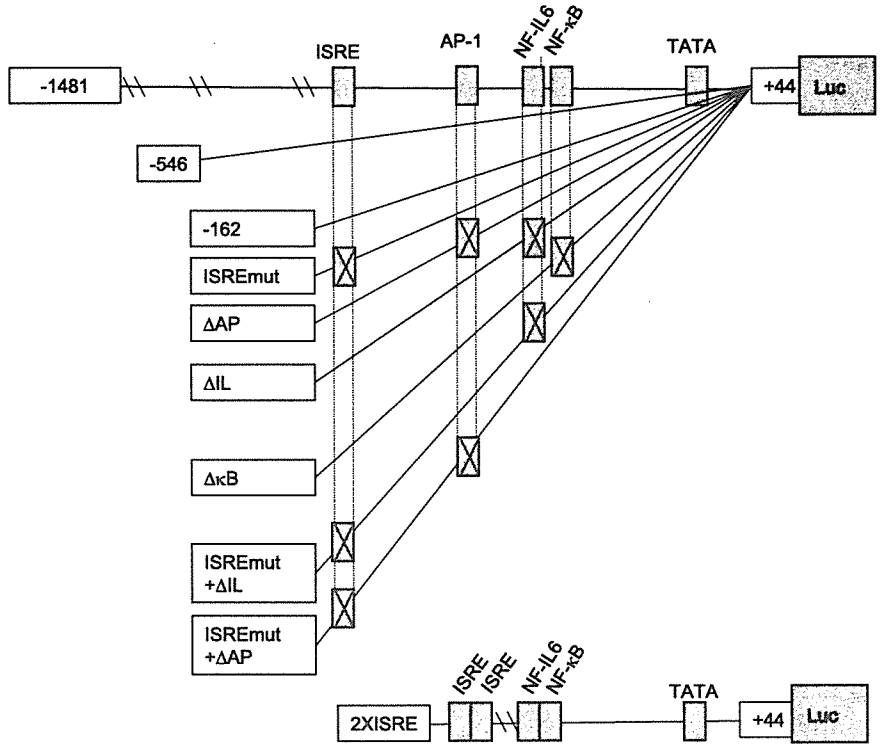

FIG. 1. Schematic representation of the CXCL-8 promoter. Locations of ISRE, AP-1, NF-IL-6, NF-κB sites are indicated. The names of the reporter constructs are found in the boxes to the left of each schematic. Luc, luciferase.

GAACAGTGTCGCCTACTACCTG), where F and R designate forward and reverse primers.

These primer sets hybridize to regions 1302 to 1473 of the genomic clone of CXCL-8 (NCBI accession number M28130) and to regions 97 to 348 of the IFN-β (NCBI accession number V00534.1) promoter and generate PCR products of 171 (CXCL-8) and 251 (IFN-β) base pairs. Forty-five cycles of PCR were performed as follows: 94°C for 15 seconds, 55°C for 30 seconds, and 72°C for 30 seconds.

Cloning and reporter studies with the CXCL-8 3′UTR. A 237-base pair region (nucleotides 972 to 1209 of accession number NM000584) from the 1,250-base pair CXCL-8 3′ untranslated region (3′UTR) was amplified by RT-PCR. Briefly, total RNA was extracted by Tri Reagent (Molecular Research Center, Cincinnati, OH) from a THP-1 monocytic cell line (ATCC, Manassas, VA) that was previously stimulated with 10 μg/ml lipopolysaccharide in the presence of cycloheximide (5 μg/ml). cDNA was synthesized and amplified by PCR with the forward primer with a BamHI site (underlined), 5′ GCACCGGATCCGATGT TGTGAGGACATGTG 3′, and the reverse primer with an XbaI site (underlined), 5′ GCCAGTCTAGAACCCTGATTGAAATTTAT 3′. The additional 5′ sequences provided thermal stability to the oligonucleotides and facilitated the restriction digest. The PCR products were purified by phenol-chloroform extraction, followed by ethanol precipitation. The PCR products were cut by BamHI and XbaI sequentially, followed by phenol extraction and ethanol precipitation. The digested PCR products were ligated into an expression vector derived from a gWIZ plasmid (Gene Therapy Systems, Inc., San Diego, CA) that contains an enhanced GFP (EGFP) coding region under the constitutive expression of the CMV/intron A promoter and has a bovine growth hormone 3′UTR. Recombinant colonies were verified by PCR using a forward vector-specific primer and a CXCL-8 3′UTR reverse primer.

Cells (3×10^4 cells per well) in black clear-bottomed 96-well plates were transfected with the GFP plasmids. Transfections were performed as mentioned above. All transfections were performed in quadruplicate. The variance in GFP fluorescence among replicate microwells was <7%. Transfection efficiency in HEK293 was always 70% ± 5%. Data are presented as the mean values ± standard errors of the fluorescence intensity determined by using a ZENYTH 3100 model instrument with the following parameters: excitation filter, 485 nm; emission filter, 535 nm; integration time, 1s; and bottom fluorescence read setting.

Statistics. Differences between means of triplicate or quadruplicate samples of luciferase or fluorescence readings were compared using Student's *t* test. A *P* value of <0.05 was considered significant.

RESULTS

Figure 1 shows a schematic representation of the CXCL-8 promoter constructs used in this study. The figure shows the full-length (−1481) and truncated (−546 and −162) promoters used in this study. The −162 construct was also altered so that the ISRE, AP-1, NF-IL-6, and NF-κB binding sites were mutated to prevent transcription factor binding (8). The 2XISRE construct contains two copies of the ISRE site fused upstream to a minimal CXCL-8 promoter containing the NF-IL-6 and NF-κB binding sites, which was shown previously to be induced by RSV infection (8).

dsRNA sensor proteins activate CXCL-8 transcription. RIG-I and related CARD-containing cellular proteins have been shown to lead to NF-κB and IRF-3 activation following viral infection or dsRNA stimulation (14, 38, 55, 66). We first demonstrated the functionality of the RIG-WT, RIG-N (constitutively active), and RIG-C (dominant negative) proteins in our experimental system. Wild-type and mutant RIG-expressing plasmids were transfected along with the IFN-β luciferase reporter gene and transfected with poly(I:C), a synthetic source of dsRNA. RIG-WT transfection led to IFN-β transcription only following dsRNA transfection, while RIG-N induced IFN-β transcription independently of dsRNA. In contrast, RIG-C inhibited IFN-β transcription under all conditions (data not shown). We also verified the expression of the RIG-WT and RIG-N proteins (Fig. 2A). We then investigated

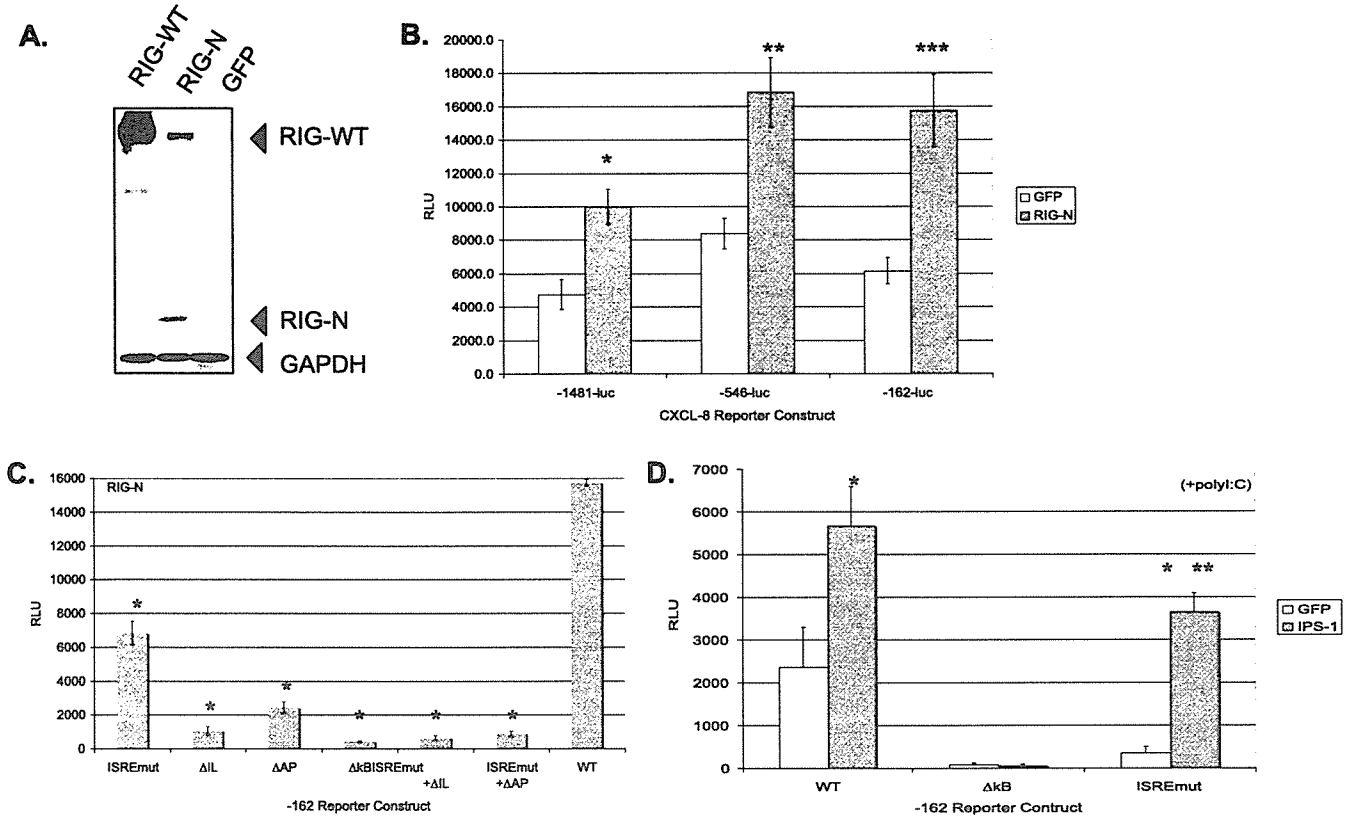

FIG. 2. Double-stranded RNA signaling pathways activate CXCL-8 transcription. (A) Expression of RIG-WT and constitutively active RIG-N proteins. Huh7 cells were transfected with plasmids expressing RIG-WT, RIG-N, or GFP, and whole-cell protein extracts were harvested 48 h later and analyzed by Western blotting with a polyclonal antiserum to RIG-I. Positions of the proteins are indicated with arrowheads. GAPDH (glyceraldehyde-3-phosphate dehydrogenase) cellular protein expression verified equal loading of proteins among the different conditions. (B) RIG-N activates CXCL-8 transcription. Huh7 cells were transfected with RIG-N- or GFP-expressing plasmids along with CXCL-8 reporter genes −1481-luc, −546-luc, or −162-luc, and luciferase readings were measured 24 h posttransfection. RLU, relative light units. Asterisks indicate significance of RIG-N luciferase values versus GFP values (*, $P = 0.002$; **, $P = 0.017$; ***, $P = 0.003$). (C) CXCL-8 promoter mutagenesis. Huh7 cells were transfected with RIG-N or GFP plasmids and the indicated CXCL-8 promoter constructs in the −162 backbone containing various mutations in transcription factor binding sites. Luciferase readings were measured 24 h posttransfection. Asterisks indicate that the luciferase values of mutant promoters compared to that of the wild-type −162 construct were significantly different (P, <0.01). (D) IPS-1 activates CXCL-8 transcription. Huh7 cells were transfected with IPS-1- or GFP-expressing plasmids along with wild-type −162 or mutant −162 promoters containing mutations in the NF-κB and ISRE binding sites, and 20 h posttransfection, cells were transfected with poly(I:C). Luciferase readings were measured 6 h later. The single asterisk indicates that IPS-1 luciferase readings were significantly different from the GFP readings (*, P <0.01). The double asterisk indicates that IPS-1-induced luciferase values from the ISRE mutant promoter were significantly lower than IPS-1 induced luciferase values from the wild-type promoter (**, $P = 0.008$).

whether RIG-I modulated CXCL-8 transcription. Huh7 cells were transfected with various CXCL-8 reporter gene constructs in the presence of constitutively active RIG-N or GFP as a negative control. As shown in Fig. 2B, RIG-N transactivated full-length (−1481) and truncated (−546 and −162) CXCL-8 promoter constructs by 2.1-, 2.0-, and 2.6-fold, respectively, relative to that of GFP (all P values were <0.02).

Because dsRNA signaling activates both IRFs and NF-κB and these transcription factors are involved in CXCL-8 induction, we examined the RIG-N activation of CXCL-8 transcription from the −162 constructs containing various mutations in their transcription factor binding sites. As shown in Fig. 2C, RIG-N activated the −162 construct, while the mutation of the ISRE caused a 2.3-fold reduction in luciferase activity (P, <0.01). Mutations of the AP-1, the NF-IL-6, and the NF-κB sites led to 6.5-, 14.8-, and 37.2-fold reductions, respectively, in transcription, while mutations of both the ISRE/NF-IL-6 and the ISRE/AP-1 sites caused 24.3- and 17.6-fold reductions, respectively, in transcription. The data indicate a requirement for NF-κB, NF-IL-6, and AP-1 in RIG-N-mediated induction of CXCL-8 transcription, with a subtle yet consistent regulation by transcription factors binding to the ISRE of the CXCL-8 promoter.

Since IPS-1 is an essential adaptor protein in RIG-I signaling (27, 38, 52, 63), we determined whether it regulates CXCL-8 transcription. Cells were transfected with reporter and expression plasmids and then transfected with poly(I:C) to provide dsRNA. As shown in Fig. 2D, IPS-1 expression activated CXCL-8 transcription from the wild-type −162 construct 2.4-fold compared to that of GFP (P, <0.01), and a mutation of the NF-κB binding site abrogated the response. A mutation of the ISRE binding site in the CXCL-8 promoter revealed that while IPS-1 still stimulated transcription 10.2-fold relative to that of GFP ($P < 0.01$), the relative levels of transcription

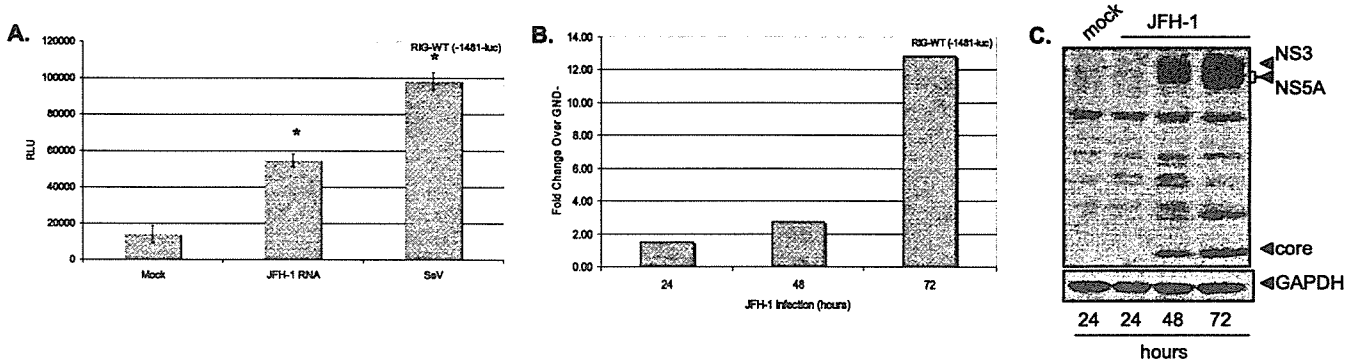

FIG. 3. HCV RNA and HCV infection activate CXCL-8 transcription. (A) Huh7.5.1 cells were transfected with RIG-WT and the full-length −1481 CXCL-8 luciferase construct, and 24 h later, cells were mock transfected, transfected with JFH-1 RNA, or infected with Sendai virus (SeV) at 100 hemagglutinin inhibitor units. Luciferase readings were measured 24 h later. Asterisks indicate that JFH-1- or Sendai virus-induced CXCL-8 transcription was significantly higher than mock-transfected cells (*, $P < 0.01$). RLU, relative light units. (B) Huh7.5.1 cells were transfected with RIG-WT and the full-length −1481 CXCL-8 luciferase construct, and 24 h later, cells were infected with JFH-1 virus stocks at an MOI of 0.01. Control cells were incubated with an equivalent volume of supernatants from cells transfected with replication-incompetent JFH-1 RNA containing the GND mutation in the viral polymerase. Luciferase readings were taken at the indicated times. Data are expressed as the increase (*n*-fold) in luciferase values over that of the GND control. (C) Western blot detection of HCV NS3, NS5A, and core proteins in Huh7.5.1 cells infected with JFH-1 at an MOI of 0.01. Blots were also probed with GAPDH (glyceraldehyde-3-phosphate dehydrogenase) to verify equal protein loading.

were 1.6-fold lower than that of the wild-type CXCL-8 promoter ($P = 0.008$). In the absence of dsRNA, IPS-1 still activated transcription from the −162 wild-type construct (data not shown). The data indicate that IPS-1 and RIG-I signal to induce the CXCL-8 promoter and that in addition to the well-known role for NF-κB, ISRE-binding proteins also regulate CXCL-8 transcription.

HCV RNA and JFH-1 infection activate CXCL-8 transcription. Huh7.5.1 cells are defective in dsRNA signaling due to a mutation in RIG-I (55). Therefore, to investigate the effect of transfection of HCV RNA on CXCL-8 transcription, cells were first cotransfected with RIG-WT and the full-length CXCL-8 promoter-luciferase construct and then transfected with JFH-1 viral RNA derived from in vitro transcription. As shown in Fig. 3A, JFH-1 RNA caused a fourfold increase in transcription from the full-length CXCL-8 promoter compared to that of the mock-transfected cells (P, <0.01). As a positive control, cells were infected with Sendai virus, which caused a sevenfold induction of CXCL-8 transcription (P, <0.01). Moreover, as shown in Fig. 3B, when Huh7.5.1 cells were transfected with RIG-WT, followed by JFH-1 virus infection, a progressive increase in CXCL-8 transcription was observed over time. Figure 3C shows the relative levels of HCV NS3, NS5A, and core proteins by Western blotting at 24, 48, and 72 h postinfection, respectively. Collectively, the data indicate that HCV infection activates CXCL-8 transcription via the RIG-I pathway. Note also that transfection of synthetic dsRNA in the form of poly(I:C) also induced CXCL-8 in a RIG-I dependent fashion (data not shown). Thus, the response is not necessarily specific to HCV RNA but may reflect a general cellular response to dsRNA exposure.

IRF-3 stimulates CXCL-8 transcription. IRF-3 has been shown to regulate the expression of other chemokines such as RANTES (32) and is central to the host's control of HCV infection (15). Since RIG-I signals to IRF-3 (66), we investigated the effects of IRF-3 expression on CXCL-8 transcription and HCV replication. Under basal conditions, IRF-3 induced a highly significant 8.5-fold increase (P, <0.01) in transcription from the full-length −1481 CXCL-8 promoter, while IRF-3 induced a 2.5-fold increase (P, <0.01) in CXCL-8 promoter activity in the presence of TNF-α (Fig. 4A). Shown below Fig. 4 A is a Western blot verifying the specific expression of IRF-3. Moreover, IRF-3 induced a statistically significant dose-dependent increase in activation of the 2XISRE CXCL-8 reporter construct (P, <0.01) (Fig. 4B). IRF-3-5D, a constitutively active mutant of IRF-3 (33), also activated the 2XISRE promoter construct (data not shown). The data indicate that IRF-3 transactivates the CXCL-8 promoter and are consistent with a recent report that during the early course of HCV infection, IRF-3 is activated (34).

IRF-3 binds directly to the CXCL-8 promoter in vivo. Since IPS-1 and RIG-I signaling to the CXCL-8 promoter requires the ISRE at positions −130 to −162 (Fig. 2C and 2D) and IRF-3 transactivates the CXCL-8 promoter (Fig. 4), we questioned whether IRF-3 binds directly to the CXCL-8 promoter. To investigate this issue, we established ChIP assays which measure binding of transcription factors to DNA in a cellular context. We first demonstrated that NF-κB, a central player in both CXCL-8 (42) and IFN-β (20) transcription, bound to the CXCL-8 and IFN-β promoters in response to double-stranded RNA transfection (Fig. 5A). The interaction was specific since CXCL-8- and IFN-β-specific amplification products were obtained only with extracted genomic DNA, input DNA, and DNA-protein complexes that were immunoprecipitated with anti-NF-κB antiserum. The data indicate that dsRNA treatment results in NF-κB activation and binding to the CXCL-8 and IFN-β promoters. Similarly, when Huh7 cells were transfected with IRF-3, the protein bound specifically to both the CXCL-8 and the IFN-β promoters (Fig. 5B). Cumulatively, the data indicate that dsRNA activates the RIG-I pathway to induce CXCL-8 transcription, which involves the binding of IRF-3 and NF-κB to the CXCL-8 promoter.

RIG-N stabilizes CXCL-8 mRNA in an ARE-dependent manner. In addition to transcriptional activation, modulation of the half-life of CXCL-8 mRNA plays a major role in CXCL-8 induction in response to various stimuli. For example,

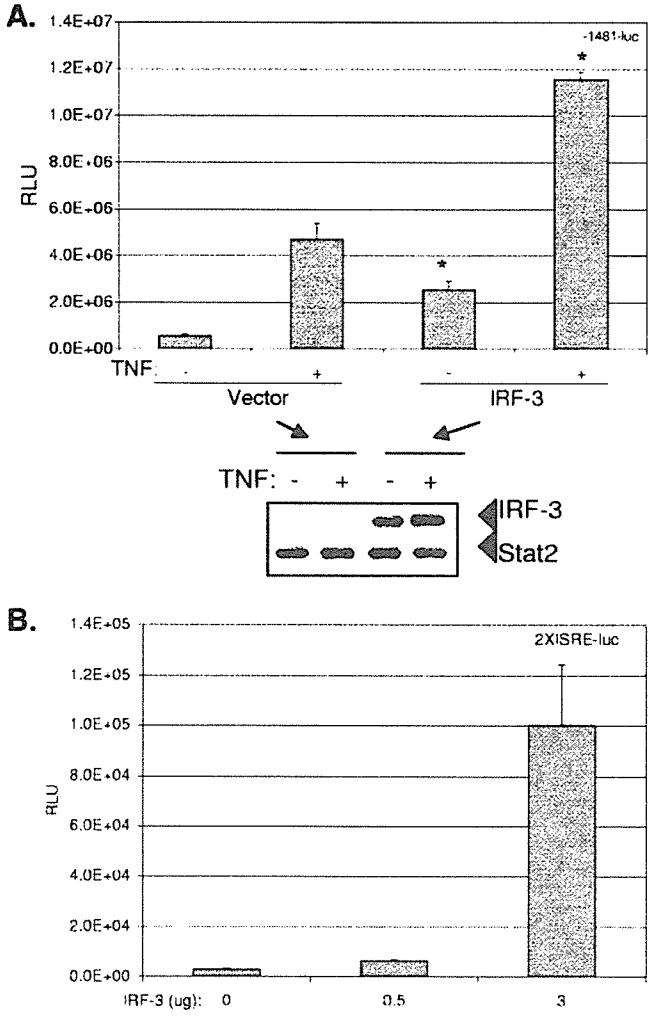

FIG. 4. IRF-3 transactivates the CXCL-8 promoter. (A) Huh7 cells were plated in 12-well plates and transfected with 0.5 μg of CMV-IRF-3 or vector plasmids along with 0.5 μg of the full-length −1481-luc CXCL-8 promoter-luciferase plasmid. Twenty-four hours later, cells were treated or not treated with 15 ng/ml of rhTNF-α for 6 h before luciferase activity was measured on cell lysates. The Western blot below the graphs depicts the expression of IRF-3 detected with polyclonal antiserum. Stat2 was also detected with polyclonal antiserum and served as a control for equal loading. Asterisks indicate significant stimulation of CXCL-8 transcription by IRF-3 compared to that of the vector control (*, $P < 0.01$). RLU, relative light units. (B) Increasing amounts of IRF-3 were cotransfected with 0.5 μg of the synthetic CXCL-8 promoter, 2XISRE-luc, into Huh7 cells, and cells and lysates were processed as described above.

TNF-α and virus induction of CXCL-8 involve mRNA stabilization (19, 23, 31, 61) via the binding of regulatory proteins to AREs in the 3′UTR of the mRNA (1, 6, 9, 53). We therefore determined whether RIG-I induction of CXCL-8 also involves stabilization of CXCL-8 mRNA. Huh7 cells were transfected with plasmids expressing RIG-N or GFP and treated with TNF-α to induce CXCL-8 mRNA. Actinomycin D was added to cultures to stop transcription, and CXCL-8 mRNA was quantified by real-time RT-PCR (19). As shown in Fig. 6A, expression of RIG-N led to a 7.6-fold enhancement of basal CXCL-8 mRNA (P, <0.01). Furthermore, RIG-N expression was associated with a 2.1-fold increase in the half-life of CXCL-8 mRNA following TNF-α stimulation. Statistical comparison of the decay rates by a one-phase exponential model (19) showed that this difference is significant ($P = 0.03$).

Since AREs are involved in the posttranscriptional regulation of CXCL-8 mRNA, we performed experiments with an EGFP reporter gene fused to the ARE region of CXCL-8 (Fig. 6B). The CXCL-8 construct contained 237 nucleotides from the CXCL-8 3′UTR that included the ARE (60). A control vector included a sequence of 200 nucleotides which lacked AREs. The CXCL-8 ARE caused a sixfold reduction in EGFP fluorescence compared to that of the wild-type vector (Fig. 6C, compare open bars). Fluorescence levels correlated with mRNA levels as detected by quantitative PCR (data not shown), indicating that the GFP reporter system reflects mRNA changes. Cotransfection experiments with RIG-N demonstrated that RIG-N was able to increase EGFP fluorescence by threefold in the presence of the CXCL-8 ARE compared to that of the wild-type vector that did not contain the ARE (Fig. 6C, solid bars). Overall, these results indicate that RIG-N stabilized CXCL-8 mRNA via ARE-dependent pathways.

DISCUSSION

The inflammatory response to virus infection, which is usually beneficial to the host, is often deregulated in the context of chronic viral infections like those caused by HCV. Indeed, inductions of inflammatory cytokines and chemokines such as CXCL-6, CXCL-8, and TNF-α have been reported in patients with chronic hepatitis C (11, 13, 18, 39, 51). In this case, the inflammatory response may do more harm than good because deregulation of inflammatory cytokines and chemokines creates an environment within the liver that is harsh and leads to hepatocyte turnover and regeneration (7, 17, 35, 37, 57). It has been suggested that chronic inflammation is mechanistically involved in the establishment of cancer (41), in particular hepatocellular carcinoma (5), so a deregulated inflammatory response may also have severe pathological sequelae.

In the current report, we demonstrate that innate antiviral signaling pathways that sense dsRNA during virus infection also trigger inflammatory chemokine expression. RIG-I and IPS-1 induced CXCL-8 transcription, and this involved, as expected, NF-κB. A role for the ISRE site in the CXCL-8 promoter was defined, and we demonstrated for the first time that IRF-3, which is downstream of RIG-I and IPS-1, also activated CXCL-8 transcription by directly binding to the CXCL-8 promoter. Moreover, RIG-N stabilized CXCL-8 mRNA. We propose that the regulation of CXCL-8 production by dsRNA signaling pathways represents a link between innate antiviral and inflammatory pathways. Based on previous studies (24, 50), HCV NS5A and core proteins could also play a role in the CXCL-8 induction observed in the present study. In this case, the mechanisms involved could be independent of dsRNA signaling responses and involve other transcription factors such as NF-κB and AP-1, reflecting the classical mode of CXCL-8 induction.

CXCL-8 induction requires transcriptional activation of the CXCL-8 promoter. Formation of the CXCL-8 "enhanceosome" involves the coordinated assembly of multiple transcrip-

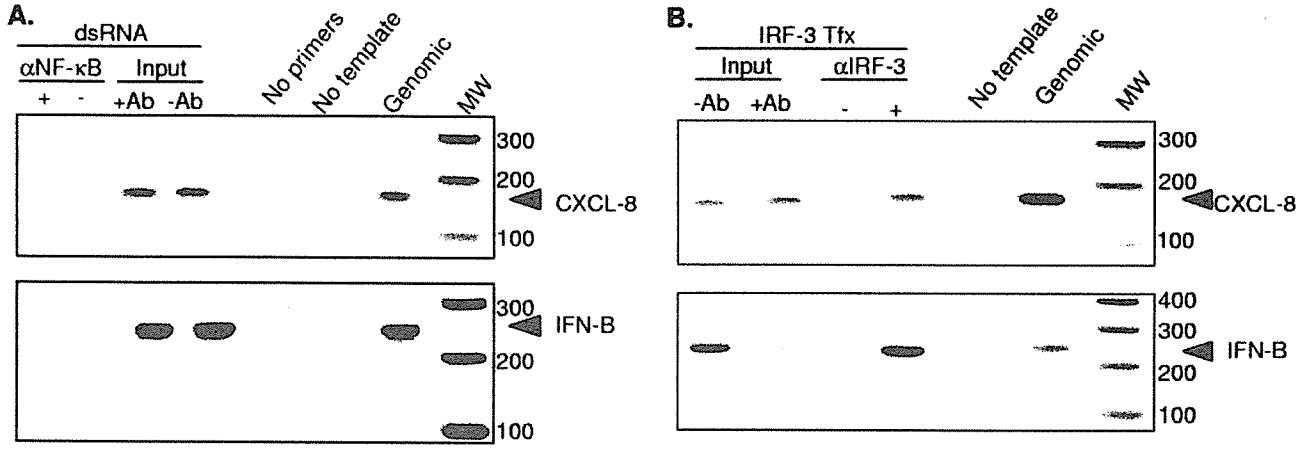

FIG. 5. IRF-3 binds directly to the CXCL-8 promoter in vivo. (A) A confluent 10-cm dish of Huh7 cells was transfected with 20 μg of poly(I:C) for 6 h. Nuclear DNA was isolated from fixed cells and sheared by sonication, and equal amounts were added to immunoprecipitations (IP) with (+) or without (−) antiserum to NF-κB. DNA was extracted from IP, and the CXCL-8 and IFN-β promoters were amplified by PCR. The PCR-positive control was genomic DNA, while PCR-negative controls contained either no primers or no template DNA. Positive controls for the IP included aliquots of the input samples that went into each IP (+antibody [Ab] or −Ab). (B) Huh7 cells were transfected with CMV-IRF3, and 24 h later, nuclear DNA was isolated from fixed cells as described above. Samples were handled as described above except polyclonal antiserum to IRF-3 was used in the immunoprecipitation. Arrows indicate the location of the CXCL-8- and IFN-β-specific PCR products.

tion factors (22). Under basal conditions, the CXCL-8 promoter is repressed by at least three mechanisms, including the binding of NF-κB repressing factor to a region that overlaps the NF-κB binding site, the deacetylation of histone proteins by histone deacetylase I (HDAC1), and the binding of octamer-1 (OCT-1) to a complementary site of the CAAT/enhancer-binding protein (C/EBP) binding sites (22). During transcriptional activation, NF-κB enters the nucleus and displaces NRF, OCT-1 is replaced by C/EBP, and CREB-binding protein (CBP)/p300 is recruited, which causes histone acetylation and remodeling of chromatin. In the current report, we demonstrate that NF-κB, AP-1, NF-IL-6, and IRF-3 participate in CXCL-8 transcriptional induction in response to HCV infection. Our data indicate that similar to RSV, HCV induces multiple transcription factors to bind to the CXCL-8 promoter. In other systems, NF-κB binding is essential to CXCL-8 transcriptional induction (42). AP-1, C/EBP, and NF-IL-6 are not required for transcriptional activation in some cells (22, 42), so it is thought that these transcription factors provide maximal gene induction. An important, unresolved issue is whether AP-1 and NF-IL-6 involvement in CXCL-8 induction requires the activation of AP-1 and NF-IL-6 signaling pathways or whether these transcription factors are noninducible and simply serve to amplify the effect of inducible IRF-3 and NF-κB. For example, it has been demonstrated that while the CXCL-8 AP-1 site is not TNF-α inducible, a mutation of the site significantly reduced TNF-α induction of the native CXCL-8 promoter (58).

RIG-I signaling is central for triggering the host response to HCV infection (34). It has been demonstrated that the HCV NS3 protease blocks RIG-I-dependent signaling of IRF-3 and NF-κB activation by its targeted proteolysis of IPS-1 (10, 34, 38). However, the host response may be transiently induced during early points of HCV infection prior to control by NS3/4A (34). Our data now indicate that the RIG-I pathway signaling through IPS-1 can also drive the expression of CXCL-8, thus connecting innate defense signaling to the inflammatory response to virus infection. We found that IRF-3 and NF-κB participate to induce CXCL-8 expression, suggesting that HCV might impose a similar blockade on CXCL-8 induction. We also note that among other transcription factors, NF-κB is essential for CXCL-8 induction and is responsive to many inflammatory stimuli other than dsRNA or virus infection (22). Thus, it is possible that viral triggering and control of CXCL-8 induction will depend on the cumulative and time-dependent cross-talk among signaling networks that is triggered and activated by NF-κB during HCV infection, with the subtle modulation imposed by the dsRNA activation of RIG-I signaling to IRF-3 serving to fine tune the response. Furthermore, while it has been suggested that IPS-1 mediates the bifurcation of the NF-κB and IRF-3 activation pathways, it remains possible that other adaptors of the RIG-I pathway are involved in this process (21).

Although transcriptional activation often plays a central role in gene expression, in certain situations, mRNA stabilization plays a more prominent role (1, 28). For instance, collagen expression in hepatic stellate cells is increased primarily through mRNA stabilization (54). Moreover, we have recently shown that Huh7 and replicon cells constitutively express CXCL-8 mRNA that is regulated posttranscriptionally (19). In the current study, we showed that RIG-N stabilized CXCL-8 mRNA, suggesting that a consequence of dsRNA signaling includes the activation of mRNA stabilizing responses. Note, however, that while ARE-mediated pathways primarily regulate mRNA turnover, they may also influence translation. However, it is likely that the RIG-N effect described in the current report acts at the mRNA level, since the half-life of CXCL-8 was prolonged as demonstrated by the actinomycin D chase experiment. The mRNA stabilization was dependent on AREs in the 3′UTR, since RIG-N increased reporter activity from a vector containing the 3′UTR region that harbors CXCL-8 AREs but not with a 3′UTR that lacked AREs. The

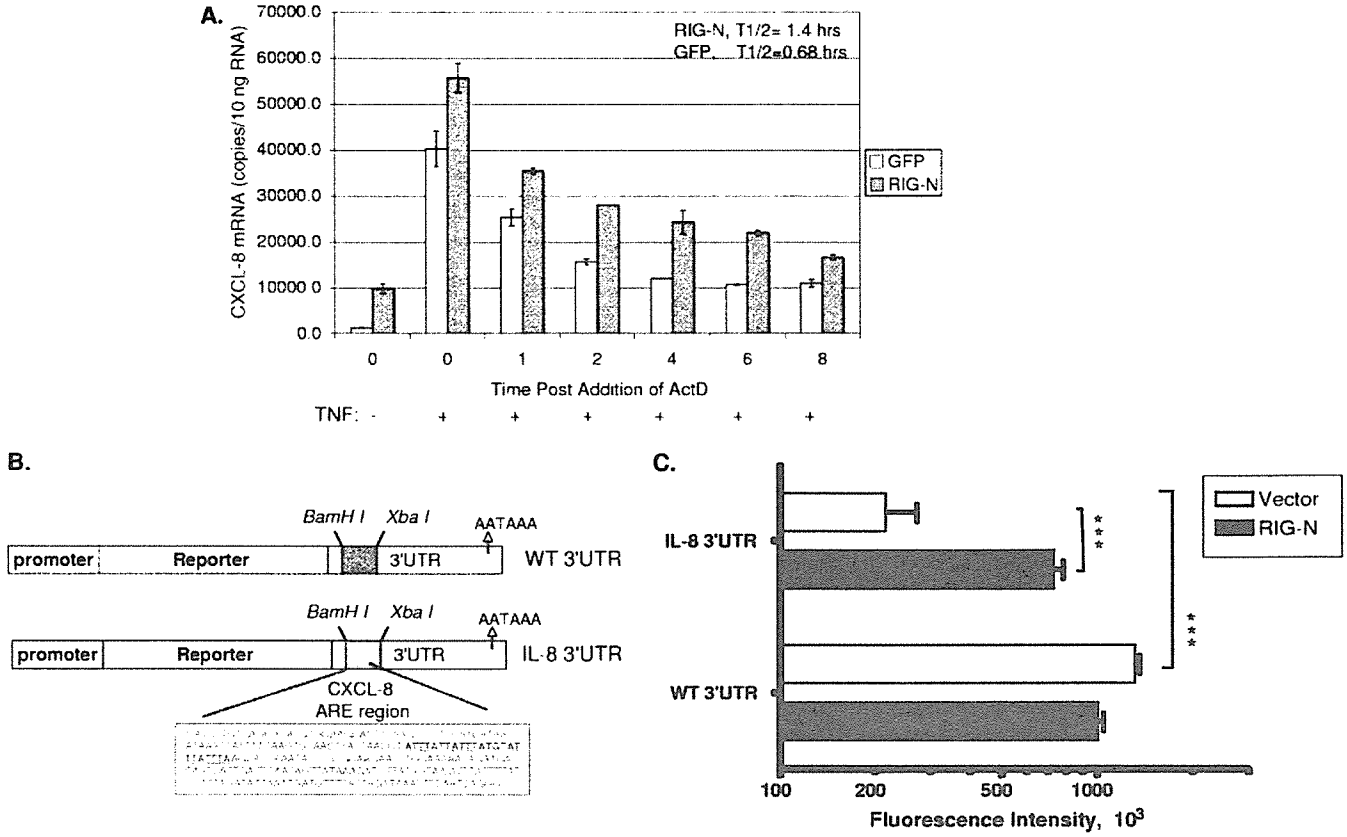

FIG. 6. RIG-N stabilizes CXCL-8 mRNA. (A) Huh7 cells were transfected with RIG-N- or GFP-expressing plasmids, and 24 h later, cells were treated with 10 ng/ml TNF-α for 2 h to induce CXCL-8 mRNA. Actinomycin D was then added to cell cultures to stop transcription, and total cellular RNA was isolated at the indicated times. CXCL-8 mRNA was quantitated by real-time RT-PCR, as described in Materials and Methods. (B) Schematic representation of the CXCL-8 ARE reporter genes. The EGFP protein was placed under the control of a constitutively active CMV promoter. The control of mRNA stability was mediated by sequences in the 3′UTR. The dashed box indicates a 200-nucleotide stuffer sequence which lacks AREs in the vector construct or 237 nucleotides from the CXCL-8 3′UTR that contains AREs. Underlined are the ARE pentamers (AUUUA). (C) Cells (3×10^4 cells per well) in black clear-bottomed 96-well plates were cotransfected with 25 ng of EGFP reporter vectors (CXCL-8 and WT) and 50 ng of modulator vectors (vector and RIG-N). After 48 h, the plates were read by bottom fluorescence. Data are presented as the means ± standard errors of four readings. ***, P values <0.001 using Student's t test.

CXCL-8 ARE was able to destabilize the reporter activity in the absence of any modulator but also was able to respond to RIG-N-induced stabilization. Thus, this region contains the necessary ARE regulatory and accessory domains for both destabilization and RIG-N-induced stabilization. This region has been shown to contain two functionally different domains in which four AUUUA-containing domains are sufficient for p38 mitogen-activated protein kinase-induced stabilization (60). Thus, it is possible that RIG-N induces the p38 pathway via a yet-unknown process. Since CXCL-8 mRNA stabilization involves the binding of regulatory proteins to the 3′UTR of the mRNA that enhance its mRNA stability (22), it is possible that RIG-N modulates the activity of these proteins. We are currently evaluating these issues. Furthermore, TLR5 and TLR9 signaling results in CXCL-8 induction by increasing the stability of CXCL-8 mRNA (46, 67). The degree to which dsRNA pathways, both TLR3 dependent and independent, regulate CXCL-8 mRNA stability during virus infection requires further study.

In summary, we have shown that dsRNA antiviral pathways cross-talk with inflammatory pathways. The combined action of these pathways is central to the control of acute HCV infection and replication. However, because HCV disrupts antiviral and inflammatory pathways (26, 48), these virus-host interactions likely contribute to HCV persistence and the pathogenesis of HCV-associated liver disease.

ACKNOWLEDGMENTS

We thank Francis Chisari, Michael David, John Hiscott, Naofumi Mukaida, and Apath, LLC, for reagents, Benjamin tenOever and Tom Maniatis for technical advice on ChIP assays, and Latifa Al-Haj, Paula McPoland, Jodie Powdrill, and Jeremiah Eng for technical assistance.

S.J.P. is partially supported by NIH grants DK62187 and U19AI66328, A.R.B. by grants AI40218 and AI062885, and M.G. by grants AI060389 and U19AI40035. T.W. is supported by grants from the Japanese Ministry of Health, Labor, and Welfare; the Japan Society for the Promotion of Science; and the Japan Health Science Foundation.

REFERENCES

1. **Bakheet, T., M. Frevel, B. R. G. Williams, W. Greer, and K. S. A. Khabar.** 2001. ARED: human AU-rich element-containing mRNA database reveals an unexpectedly diverse functional repertoire of encoded proteins. Nucleic Acids Res. **29**:246–254.

2. **Barnes, B., B. Lubyova, and P. M. Pitha.** 2002. On the role of IRF in host defense. J. Interferon Cytokine Res. **22:**59–71.
3. **Bonte, D., C. Francois, S. Castelain, V. Morel, J. Roussel, C. Wychowski, J. Dubuisson, E. Meurs, and G. Duverlie.** 2002. Induction of the IL-8 chemokine by the hepatitis C virus NS5A nonstructural protein in an infectious system. Hepatology **36:**A495.
4. **Bonte, D., C. Francois, S. Castelain, C. Wychowski, J. Dubuisson, E. F. Meurs, and G. Duverlie.** 2004. Positive effect of the hepatitis C virus nonstructural 5A protein on viral multiplication. Arch. Virol. **149:**1353–1371.
5. **Branda, M., and J. R. Wands.** 2006. Signal transduction cascades and hepatitis B and C related hepatocellular carcinoma. Hepatology **43:**891–902.
6. **Brennan, C. M., and J. A. Steitz.** 2001. HuR and mRNA stability. Cell Mol. Life Sci. **58:**266–277.
7. **Carr, D. J., and L. Tomanek.** 2006. Herpes simplex virus and the chemokines that mediate the inflammation. Curr. Top. Microbiol. Immunol. **303:**47–65.
8. **Casola, A., R. P. Garofalo, M. Jamaluddin, S. Vlahopoulos, and A. R. Brasier.** 2000. Requirement of a novel upstream response element in respiratory syncytial virus-induced IL-8 gene expression. J. Immunol. **164:**5944–5951.
9. **Chen, C. Y., and A. B. Shyu.** 1995. AU-rich elements: characterization and importance in mRNA degradation. Trends Biochem. Sci. **20:**465–470.
10. **Cheng, G., J. Zhong, and F. V. Chisari.** 2006. Inhibition of dsRNA-induced signaling in hepatitis C virus-infected cells by NS3 protease-dependent and -independent mechanisms. Proc. Natl. Acad. Sci. USA **103:**8499–8504.
11. **Chuang, E., A. Del Vecchio, S. Smolinski, X. Y. Song, and R. T. Sarisky.** 2004. Biomedicines to reduce inflammation but not viral load in chronic HCV—what's the sense? Trends Biotechnol. **22:**517–523.
12. **Davis, G. L., J. E. Albright, S.F. Cook, and D. M. Rosenberg.** 2003. Projecting future complications of chronic hepatitis C in the United States. Liver Transplant. **9:**331–338.
13. **Falasca, K., C. Ucciferri, M. Dalessandro, P. Zingariello, P. Mancino, C. Petrarca, E. Pizzigallo, P. Conti, and J. Vecchiet.** 2006. Cytokine patterns correlate with liver damage in patients with chronic hepatitis B and C. Ann. Clin. Lab. Sci. **36:**144–150.
14. **Foy, E., K. Li, R. Sumpter, Jr., Y. M. Loo, C. L. Johnson, C. Wang, P. M. Fish, M. Yoneyama, T. Fujita, S. M. Lemon, and M. Gale, Jr.** 2005. Control of antiviral defenses through hepatitis C virus disruption of retinoic acid-inducible gene-I signaling. Proc. Natl. Acad. Sci. USA **102:**2986–2991.
15. **Foy, E., K. Li, C. Wang, R. Sumpter, Jr., M. Ikeda, S. M. Lemon, and M. Gale, Jr.** 2003. Regulation of interferon regulatory factor-3 by the hepatitis C virus serine protease. Science **300:**1145–1148.
16. **Girard, S., P. Shalhoub, P. Lescure, A. Sabile, D. E. Misek, S. Hanash, C. Brechot, and L. Beretta.** 2002. An altered cellular response to interferon and up-regulation of interleukin-8 induced by the hepatitis C viral protein NS5A uncovered by microarray analysis. Virology **295:**272–283.
17. **Glass, W. G., H. F. Rosenberg, and P. M. Murphy.** 2003. Chemokine regulation of inflammation during acute viral infection. Curr. Opin. Allergy Clin. Immunol. **3:**467–473.
18. **Gonzalez-Amaro, R., C. Garcia-Monzon, L. Garcia-Buey, R. Moreno-Otero, J. L. Alonso, E. Yague, J. P. Pivel, M. Lopez-Cabrera, E. Fernandez-Ruiz, and F. Sanchez-Madrid.** 1994. Induction of tumor necrosis factor alpha production by human hepatocytes in chronic viral hepatitis. J. Exp. Med. **179:**841–848.
19. **Green, J., K. S. Khabar, B. C. Koo, B. R. Williams, and S. J. Polyak.** 2006. Stability of CXCL-8 and related AU-Rich mRNAs in the context of hepatitis C virus replication in vitro. J. Infect. Dis. **193:**802–811.
20. **Hiscott, J., N. Grandvaux, S. Sharma, B. R. Tenoever, M. J. Servant, and R. Lin.** 2003. Convergence of the NF-kappaB and interferon signaling pathways in the regulation of antiviral defense and apoptosis. Ann. N. Y. Acad. Sci. **1010:**237–248.
21. **Hiscott, J., R. Lin, P. Nakhaei, and S. Paz.** 2006. MasterCARD: a priceless link to innate immunity. Trends Mol. Med. **12:**53–56.
22. **Hoffmann, E., O. Dittrich-Breiholz, H. Holtmann, and M. Kracht.** 2002. Multiple control of interleukin-8 gene expression. J. Leukoc. Biol. **72:**847–855.
23. **Holtmann, H., R. Winzen, P. Holland, S. Eickemeier, E. Hoffmann, D. Wallach, N. L. Malinin, J. A. Cooper, K. Resch, and M. Kracht.** 1999. Induction of interleukin-8 synthesis integrates effects on transcription and mRNA degradation from at least three different cytokine- or stress-activated signal transduction pathways. Mol. Cell. Biol. **19:**6742–6753.
24. **Hoshida, Y., N. Kato, H. Yoshida, Y. Wang, M. Tanaka, T. Goto, M. Otsuka, H. Taniguchi, M. Moriyama, F. Imazeki, O. Yokosuka, T. Kawabe, Y. Shiratori, and M. Omata.** 2005. Hepatitis C virus core protein and hepatitis activity are associated through transactivation of interleukin-8. J. Infect. Dis. **192:**266–275.
25. **Imaizumi, T., S. Aratani, T. Nakajima, M. Carlson, T. Matsumiya, K. Tanji, K. Ookawa, H. Yoshida, S. Tsuchida, T. M. McIntyre, S. M. Prescott, G. A. Zimmerman, and K. Satoh.** 2002. Retinoic acid-inducible gene-I is induced in endothelial cells by LPS and regulates expression of COX-2. Biochem. Biophys. Res. Commun. **292:**274–279.
26. **Johnson, C. L., and M. Gale, Jr.** 2006. CARD games between virus and host get a new player. Trends Immunol. **27:**1–4.
27. **Kawai, T., K. Takahashi, S. Sato, C. Coban, H. Kumar, H. Kato, K. J. Ishii, O. Takeuchi, and S. Akira.** 2005. IPS-1, an adaptor triggering RIG-I- and Mda5-mediated type I interferon induction. Nat. Immunol. **6:**981–988.
28. **Khabar, K. S.** 2005. The AU-rich transcriptome: more than interferons and cytokines, and its role in disease. J. Interferon Cytokine Res. **25:**1–10.
29. **Khabar, K. S., F. Al-Zoghaibi, M. N. Al-Ahdal, T. Murayama, M. Dhalla, N. Mukaida, M. Taha, S. T. Al-Sedairy, Y. Siddiqui, G. Kessie, and K. Matsushima.** 1997. The alpha chemokine, interleukin 8, inhibits the antiviral action of interferon alpha. J. Exp. Med. **186:**1077–1085.
30. **Koo, B. C. A., P. McPoland, J. P. Wagoner, O. J. Kane, V. Lohmann, and S. J. Polyak.** 2006. Relationships between hepatitis C virus replication and CXCL-8 production in vitro. J. Virol. **80:**7885–7893.
31. **Leland Booth, J., and J. P. Metcalf.** 1999. Type-specific induction of interleukin-8 by adenovirus. Am. J. Respir. Cell Mol. Biol. **21:**521–527.
32. **Lin, R., C. Heylbroeck, P. Genin, P. M. Pitha, and J. Hiscott.** 1999. Essential role of interferon regulatory factor 3 in direct activation of RANTES chemokine transcription. Mol. Cell. Biol. **19:**959–966.
33. **Lin, R., Y. Mamane, and J. Hiscott.** 1999. Structural and functional analysis of interferon regulatory factor 3: localization of the transactivation and autoinhibitory domains. Mol. Cell. Biol. **19:**2465–2474.
34. **Loo, Y. M., D. M. Owen, K. Li, A. K. Erickson, C. L. Johnson, P. M. Fish, D. S. Carney, T. Wang, H. Ishida, M. Yoneyama, T. Fujita, T. Saito, W. M. Lee, C. H. Hagedorn, D. T. Lau, S. A. Weinman, S. M. Lemon, and M. Gale, Jr.** 2006. Viral and therapeutic control of IFN-beta promoter stimulator 1 during hepatitis C virus infection. Proc. Natl. Acad. Sci. USA **103:**6001–6006.
35. **Mackay, C. R.** 2001. Chemokines: immunology's high impact factors. Nat. Immunol. **2:**95–101.
36. **Mamane, Y., C. Heylboreck, P. Genei, M. Algarte, M. J. Servant, C. LePage, C. DeLuca, H. Kwon, R. Lin, and J. Hiscott.** 1999. Interferon regulatory factors: the next generation. Gene **237:**1–14.
37. **Melchjorsen, J., L. N. Sorensen, and S. R. Paludan.** 2003. Expression and function of chemokines during viral infections: from molecular mechanisms to in vivo function. J. Leukoc. Biol. **74:**331–343.
38. **Meylan, E., J. Curran, K. Hofmann, D. Moradpour, M. Binder, R. Bartenschlager, and J. Tschopp.** 2005. Cardif is an adaptor protein in the RIG-I antiviral pathway and is targeted by hepatitis C virus. Nature **437:**1167–1172
39. **Mihm, S., E. Herrmann, U. Sarrazin, M. V. Wagner, B. Kronenberger, S. Zeuzem, and C. Sarrazin.** 2004. Association of serum interleukin-8 with virologic response to antiviral therapy in patients with chronic hepatitis C. J. Hepatol. **40:**845–852.
40. **Miller, K., S. McArdle, M. J. Gale, Jr., D. A. Geller, B. Tenoever, J. Hiscott, D. R. Gretch, and S. J. Polyak.** 2004. Effects of the hepatitis C virus core protein on innate cellular defense pathways. J. Interferon Cytokine Res. **24:**391–402.
41. **Moss, S. F., and M. J. Blaser.** 2005. Mechanisms of disease: inflammation and the origins of cancer. Nat. Clin. Pract. Oncol. **2:**90–97.
42. **Mukaida, N.** 2000. Interleukin-8: an expanding universe beyond neutrophil chemotaxis and activation. Int. J. Hematol. **72:**391–398.
43. **Mukaida, N., A. Harada, K. Yasumoto, and K. Matsushima.** 1992. Properties of ipronflammatory cell type-specific leukocyte chemotactic cytokines, interleukin 8 (IL-8) and monocyte chemotactic and activating factor (MCAF). Microbiol. Immunol. **36:**773–789.
44. **Mukaida, N., M. Shiroo, and K. Matsushima.** 1989. Genomic structure of the human monocyte-derived neutrophil chemotactic factor IL-8. J. Immunol. **143:**1366–1371.
45. **Murayama, T., N. Mukaida, K. S. Khabar, and K. Matsushima.** 1998. Potential involvement of IL-8 in the pathogenesis of human cytomegalovirus infection. J. Leukoc. Biol. **64:**62–67.
46. **Parilla, N. W., V. S. Hughes, K. M. Lierl, H. R. Wong, and K. Page.** 2006. CpG DNA modulates interleukin 1 beta-induced interleukin-8 expression in human bronchial epithelial (16HBE14o-) cells. Respir. Res. **7:**84.
47. **Plumlee, C. R., C. A. Lazaro, N. Fausto, and S. J. Polyak.** 2005. Effect of ethanol on innate antiviral pathways and HCV replication in human liver cells. Virol. J. **2:**89.
48. **Polyak, S. J.** 2006. Resistance of hepatitis C virus to the host antiviral response. Future Virology. **1:**89–98.
49. **Polyak, S. J., D. Paschal, S. McArdle, M. Gale, D. Moradpour, and D. R. Gretch.** 1999. Characterization of the effects of hepatitis C virus non-structural 5a protein expression in human cell lines and on interferon-sensitive virus replication. Hepatology **29:**1262–1271.
50. **Polyak, S. J., K. S. A. Khabar, D. M. Paschal, H. J. Ezelle, G. Duverlie, G. N. Barber, D. E. Levy, N. Mukaida, and D. R. Gretch.** 2001. Hepatitis C virus nonstructural 5A protein induces interleukin-8, leading to partial inhibition of the interferon-induced antiviral response. J. Virol. **75:**6095–6106.
51. **Polyak, S. J., K. S. A. Khabar, M. Rezeiq, and D. R. Gretch.** 2001. Elevated levels of interleukin-8 in serum are associated with hepatitis C virus infection and resistance to interferon therapy. J. Virol. **75:**6209–6211.
52. **Seth, R. B., L. Sun, C. K. Ea, and Z. J. Chen.** 2005. Identification and characterization of MAVS, a mitochondrial antiviral signaling protein that activates NF-kappaB and IRF 3. Cell **122:**669–682.
53. **Shaw, G., and R. Kamen.** 1986. A conserved AU sequence from the 3'

untranslated region of GM-CSF mRNA mediates selective mRNA degradation. Cell **46**:659–667.
54. **Stefanovic, B., C. Hellerbrand, M. Holcik, M. Briendl, S. A. Liebhaber, and D. A. Brenner.** 1997. Posttranscriptional regulation of collagen α1(I) mRNA in hepatic stellate cells. Mol. Cell. Biol. **17**:5201–5209.
55. **Sumpter, R., Jr., Y.-M. Loo, E. Foy, K. Li, M. Yoneyama, T. Fujita, S. M. Lemon, and M. Gale, Jr.** 2005. Regulating intracellular antiviral defense and permissiveness to hepatitis C virus RNA replication through a cellular RNA helicase, RIG-I. J. Virol. **79**:2689–2699.
56. **Thomas, D. L., J. Astemborski, R. M. Rai, F. A. Anania, M. Schaeffer, N. Galai, K. Nolt, K. E. Nelson, S. A. Strathdee, L. Johnson, O. Laeyendecker, J. Boitnott, L. E. Wilson, and D. Vlahov.** 2000. The natural history of hepatitis C virus infection—host, viral, and environmental factors. JAMA **284**:450–456.
57. **Tripp, R. A., C. Oshansky, and R. Alvarez.** 2005. Cytokines and respiratory syncytial virus infection. Proc. Am. Thorac. Soc. **2**:147–149.
58. **Vlahopoulos, S., I. Boldogh, A. Casola, and A. R. Brasier.** 1999. Nuclear factor-kappaB-dependent induction of interleukin-8 gene expression by tumor necrosis factor alpha: evidence for an antioxidant sensitive activating pathway distinct from nuclear translocation. Blood **94**:1878–1889.
59. **Wakita, T., T. Pietschmann, T. Kato, T. Date, M. Miyamoto, Z. Zhao, K. Murthy, A. Habermann, H. G. Krausslich, M. Mizokami, R. Bartenschlager, and T. J. Liang.** 2005. Production of infectious hepatitis C virus in tissue culture from a cloned viral genome. Nat. Med. **11**:791–796.
60. **Winzen, R., G. Gowrishankar, F. Bollig, N. Redich, K. Resch, and H. Holtmann.** 2004. Distinct domains of AU-rich elements exert different functions in mRNA destabilization and stabilization by p38 mitogen-activated protein kinase or HuR. Mol. Cell. Biol. **24**:4835–4847.
61. **Winzen, R., M. Kracht, B. Ritter, A. Wilhelm, C. Y. Chen, A. B. Shyu, M. Muller, M. Gaestel, K. Resch, and H. Holtmann.** 1999. The p38 MAP kinase pathway signals for cytokine-induced mRNA stabilization via MAP kinase-activated protein kinase 2 and an AU-rich region-targeted mechanism. EMBO J. **18**:4969–4980.
62. **World Health Organization and Viral Hepatitis Prevention Board, Antwerp, Belgium.** 1999. Global surveillance and control of hepatitis C. J. Viral Hepat. **6**:35–47.
63. **Xu, L. G., Y. Y. Wang, K. J. Han, L. Y. Li, Z. Zhai, and H. B. Shu.** 2005. VISA is an adapter protein required for virus-triggered IFN-beta signaling. Mol. Cell **19**:727–740.
64. **Yagita, H., T. Nakamura, H. Karasuyama, and K. Okumura.** 1989. Monoclonal antibodies specific for murine CD2 reveal its presence on B as well as T cells. Proc. Natl. Acad. Sci. USA **86**:645–649.
65. **Yamaoka, Y., T. Kudo, H. Lu, A. Casola, A. R. Brasier, and D. Y. Graham.** 2004. Role of interferon-stimulated responsive element-like element in interleukin-8 promoter in Helicobacter pylori infection. Gastroenterology **126**: 1030–1043.
66. **Yoneyama, M., M. Kikuchi, T. Natsukawa, N. Shinobu, T. Imaizumi, M. Miyagishi, K. Taira, S. Akira, and T. Fujita.** 2004. The RNA helicase RIG-I has an essential function in double-stranded RNA-induced innate antiviral responses. Nat. Immunol. **5**:730–737.
67. **Yu, Y., H. Zeng, S. Lyons, A. Carlson, D. Merlin, A. S. Neish, and A. T. Gewirtz.** 2003. TLR5-mediated activation of p38 MAPK regulates epithelial IL-8 expression via posttranscriptional mechanism. Am. J. Physiol. Gastrointest. Liver Physiol. **285**:G282–G290.
68. **Zhong, J., P. Gastaminza, G. Cheng, S. Kapadia, T. Kato, D. R. Burton, S. F. Wieland, S. L. Uprichard, T. Wakita, and F. V. Chisari.** 2005. Robust hepatitis C virus infection in vitro. Proc. Natl. Acad. Sci. USA **102**:9294–9299.

JOURNAL OF VIROLOGY, July 2006, p. 6964–6972 Vol. 80, No. 14
0022-538X/06/$08.00+0 doi:10.1128/JVI.00024-06

Hepatitis C Virus Entry Depends on Clathrin-Mediated Endocytosis

Emmanuelle Blanchard,[1] Sandrine Belouzard,[1] Lucie Goueslain,[1] Takaji Wakita,[2] Jean Dubuisson,[1] Czeslaw Wychowski,[1] and Yves Rouillé[1]*

CNRS-UMR8161, Institut de Biologie de Lille and Institut Pasteur de Lille, Lille, France,[1] and Department of Virology II, National Institute for Infectious Diseases, Tokyo, Japan[2]

Received 4 January 2006/Accepted 3 May 2006

Due to difficulties in cell culture propagation, the mechanisms of hepatitis C virus (HCV) entry are poorly understood. Here, postbinding cellular mechanisms of HCV entry were studied using both retroviral particles pseudotyped with HCV envelope glycoproteins (HCVpp) and the HCV clone JFH-1 propagated in cell culture (HCVcc). HCVpp entry was measured by quantitative real-time PCR after 3 h of contact with target cells, and HCVcc infection was quantified by immunoblot analysis and immunofluorescence detection of HCV proteins expressed in infected cells. The functional role of clathrin-mediated endocytosis in HCV entry was assessed by small interfering RNA-mediated clathrin heavy chain depletion and with chlorpromazine, an inhibitor of clathrin-coated pit formation at the plasma membrane. In both conditions, HCVpp entry and HCVcc infection were inhibited. HCVcc infection was also inhibited by pretreating target cells with bafilomycin A1 or chloroquine, two drugs known to interfere with endosome acidification. These data indicate that HCV enters target cells by clathrin-mediated endocytosis, followed by a fusion step from within an acidic endosomal compartment.

Hepatitis C virus (HCV) infects about 170 million people around the world. Despite the importance of HCV as a human pathogen, little is known about its cell biology. The virus was identified and cloned more than 15 years ago (7), but the lack of a robust system allowing for the production of HCV in cell culture has hampered for many years functional studies on HCV infection.

In recent years, two major advances have made it possible to investigate HCV entry. A first advance has been the production of infectious retroviral particles pseudotyped with HCV envelope glycoproteins (3, 14, 24). Using this system of HCV pseudoparticles (HCVpp), observations on receptor usage and the facilitating role of high-density lipoprotein during entry were reported (3, 24, 55). A second major advance has been the recent development of a cell culture model for HCV (30, 56, 59). This system allows for the production of virus that can be efficiently propagated in cell culture (HCVcc). Therefore, the cell entry of HCV can now be investigated in the context of an infectious cycle.

HCV belongs to the *Hepacivirus* genus in the *Flaviviridae* family, which also includes the *Flavivirus* and *Pestivirus* genera (31). The HCV genome encodes three structural proteins, capsid protein C and envelope glycoproteins E1 and E2, which are associated in the form of a heterodimer (13). Several cellular proteins were reported to interact in vitro with isolated E2. These putative receptors include the tetraspanin CD81 (42), the scavenger receptor class B type I (SR-BI) (50), the lectins L-SIGN and DC-SIGN (18, 32), the asialoglycoprotein receptor (49), and heparan-sulfate proteoglycans (2). The low-density lipoprotein receptor was also proposed as a candidate receptor (1). The importance of CD81 and SR-BI in HCV entry was confirmed with HCVpp (3, 4, 24) as well as with HCVcc for CD81 (30, 56). Beyond receptor binding, virtually nothing is known about molecular and cellular mechanisms used by HCV during cell entry.

According to postbinding mechanisms of entry, enveloped viruses fall into two main types. Some viruses deliver their genome to the cytosol of target cells by fusing their envelope with the plasma membrane, while other ones enter by endocytosis. For many enveloped viruses that enter cells by endocytosis, an activation step occurs in endosomes which leads to the fusion of the viral envelope with the membrane of the endosome and the delivery of the viral genome into the cytosol. The acidic pH of endosomes is thought to play an essential role in triggering this fusion event, which is catalyzed by a viral envelope glycoprotein. Therefore, the pH sensitivity is often considered a good indication of entry by endocytosis. The best documented mode of endocytosis is the clathrin-mediated pathway. However, recent studies have revealed a surprising variety of endocytic routes (10, 39, 51).

Previous reports have indicated a pH dependency for HCVpp entry (4, 24), suggesting that HCV would enter cells by endocytosis. However, the functional importance of endocytosis in HCV infection has not been directly tested so far, and the endocytic pathway used by the virus has not been identified. In this paper, we report on postbinding cellular mechanisms of HCV entry. Using both a newly developed HCVpp entry assay and the JFH1-based HCVcc model, we confirmed the pH sensitivity of HCV entry and established the functional importance of clathrin-mediated endocytosis in HCV entry.

MATERIALS AND METHODS

Chemicals. Dulbecco's modified Eagle's medium (DMEM), phosphate-buffered saline (PBS), OptiMEM, HEPES, and goat and fetal calf sera (FCS) were purchased from Invitrogen. Hoechst dye 33342 was from Molecular Probes. Chlorpromazine was from Alexis. Bafilomycin-A1 and Mowiol 3-88 were from

* Corresponding author. Mailing address: Équipe Hépatite C, CNRS-UMR8161, Institut de Biologie de Lille, 1 rue du Professeur Calmette, BP447, 59021 Lille cedex, France. Phone: (33) 3 20 87 10 27. Fax: (33) 3 20 87 12 01. E-mail: yves.rouille@ibl.fr.

Calbiochem. ExGen500 was purchased from Euromedex. All other chemicals were from Sigma.

Antibodies. Rat monoclonal antibody (MAb) 3/11 (17) and mouse MAb A4 (15) were produced in vitro by using a MiniPerm apparatus (Heraeus) as recommended by the manufacturer. Anti-NS3 (486D39) MAb was kindly provided by J. F. Delagneau (Bio-Rad, France). Mouse anti-E2 MAb AP33 (9) was kindly provided by A. H. Patel (Institute of Virology, Glasgow, United Kingdom). Mouse anti-clathrin heavy chain (CHC) MAb was purchased from BD Biosciences. Goat anti-actin polyclonal antibody and mouse anti-simian virus 40 (SV40) T-antigen MAb (Pab101 [sc-147]) were from Santa Cruz. Anti-green fluorescent protein (GFP) MAb was from Roche. Alexa594-conjugated or Alexa555-conjugated goat anti-mouse secondary antibody was from Molecular Probes.

Cell culture. 293T human embryo kidney cells (HEK 293T), PLC/PRF/5 human hepatoma cells (ATCC CRL-8024), and Huh-7 human hepatoma cells were grown in Dulbecco's modified essential medium supplemented with glutamax and 10% fetal bovine serum.

Production of HCVpp. Pseudotyped particles were produced as described previously (3). Plasmids were kindly provided by D. Lavillette, B. Bartosch, and F.-L. Cosset (INSERM U412, Lyon, France). Briefly, 293T cells were cotransfected with a murine leukemia virus (MLV)-based transfer vector encoding luciferase (37), a murine leukemia virus Gag-Pol packaging construct, and an envelope glycoprotein-expressing vector, phCMV-E1E2 (3), using Exgen 500 as recommended by the manufacturer. The phCMV-G, phCMV-RD114, phCMV-A, and phCMV-HA expression vectors encode the vesicular stomatitis virus G protein (VSV-G), the feline endogenous virus RD114 glycoprotein, the MLV 10A1 envelope glycoprotein (A-MLV), and the fowl plague virus H7 hemagglutinin (HA), respectively (48). The phCMV-NA expression vector for influenza virus neuraminidase (NA) was a kind gift from F.-L. Cosset. Pseudotyped particles harboring VSV-G, RD114, A-MLV, or hemagglutinin (HA) and NA envelope glycoproteins on murine leukemia virus cores (VSV-Gpp, RD114pp, A-MLVpp, and HA/NApp, respectively) were used as controls. Supernatants containing the pseudotyped particles were harvested 48 h after transfection, filtered through 0.45-μm-pore-sized membranes, and incubated with 300 U/ml DNase I (Roche) for 30 min at 37°C to remove excess plasmid DNA. Pseudotyped particle stocks were kept at 4°C and used within 1 week after production. The luciferase-based HCVpp infection assay was as previously described (37).

PCR-based entry assay. Confluent cell monolayers grown in 12-well plates were infected with 600 μl of DNase-treated pseudoparticles in DMEM supplemented with 10% FCS and 20 mM HEPES. The multiplicity of infection was about 1 (range, 0.5 to 1.5). The infection was enhanced by spinoculation, as previously reported for human immunodeficiency virus (36). Plates were enclosed in plastic bags and centrifuged at 1,200 × *g* for 2 h at 37°C and then incubated for 1 h in a 5% CO_2 incubator at 37°C. After 3 h of contact, the cells were washed three times with PBS. Total DNA was extracted using the Wizard SV Genomic DNA Purification System (Promega) according to the manufacturer's instructions. Each sample of DNA was purified from two pooled wells and was dissolved into 200 μl of DNase-free water.

Quantification of early reverse-transcribed viral DNA was performed by quantitative PCR assay. Primers were designed in the U3 region of the long terminal repeat (LTR) of MLV with the help of the Primer3 software (45). The sequences of the forward and reverse U3 primers were 5′-CCATCAGATGTTTCCAGGC T-3′ and 5′-GCGACTCAGTCTATCGGAGG-3′, respectively. DNA was amplified in glass capillaries using a LightCycler instrument (Roche Diagnostics, Meylan, France). The PCR mix contained 4 μl of sample DNA and 16 μl of FastSTART DNA Master SYBR Green I (Roche Diagnostics), 4 mM $MgCl_2$, and 0.5 μM of each primer. The PCR amplification was performed for 40 cycles of 15 s at 95°C, 5 s at 60°C, and 7 s at 72°C. The specificity of the amplicon was determined by using melting curve analysis, which displayed only one peak in agreement with a specific amplicon.

The standard curves for quantification of the U3 LTR region of MLV were constructed with 10-fold serial dilutions ranging from 10^5 to 100 copies of phCMV-Luc plasmid. The standard curve was also used to assess PCR efficiency by examining its slope, which was consistently between −3.45 and −3.3 for each experiment. Individual samples were evaluated in duplicate. Absolute quantification of the viral load was evaluated by using the albumin gene as an internal control gene, as described previously (19). The conditions used to amplify the albumin gene were identical to those used for the U3 LTR region. The infection was scored as the ratio of U3 LTR DNA mean copy number over albumin DNA mean copy number. Background values obtained from parallel infections with pseudoparticles containing no envelope protein were subtracted. Data are presented as the percentage of infection relative to control conditions. Using this assay, HCVpp preparations usually yielded titers between 10^5 and 10^6 infectious units/ml on PLC/PRF/5 cells.

Production of HCVcc. To generate genomic HCV RNA, the plasmid pJFH1 (56) was linearized at the 3′ end of the HCV cDNA by XbaI digestion. Following treatment with mung bean nuclease, the linearized DNA was then used as a template for in vitro transcription with the MEGAscript kit from Ambion. In vitro-transcribed RNA was delivered to Huh-7 cells by electroporation as described previously (25). Viral stocks were obtained by harvesting cell culture supernatants at 1 week posttransfection. Secondary viral stocks were obtained by additional amplifications on naïve Huh-7 cells. Infectious titers of viral stocks were estimated between 10^5 and 10^6 infectious units per ml, based on immunofluorescent detection of infected foci following infection of Huh7 cells with serial dilutions of viral stocks.

Other viruses. The recombinant Sindbis virus expressing HCV envelope protein E1 was previously described (16). Stocks of SV40 virus were previously described (58). The recombinant Sendai virus (SeV) expressing a green fluorescent protein (GFP) was previously described (28). A purified stock of recombinant SeV was kindly provided by Laurent Roux, University of Geneva.

HCVcc infection. For HCVcc infection assays, Huh-7 cells grown in 24-well plates were infected for 2 h at 37°C with HCVcc or control viruses. Each HCVcc stock was concentrated between 5 and 10 times by ultrafiltration using Vivaspin cartridges (molecular weight cutoff, 300,000) in order to get 20 to 40% infected cells. For experiments using small interfering RNA (siRNA), equal numbers of CHC siRNA-treated cells and control siRNA-treated cells were infected. For experiments using chlorpromazine and inhibitors of endosomal acidification, cells were preincubated with inhibitors for 30 min before infection, and the drugs were added to the infection and culture media up to the end of the experiment. In some control experiments, drugs were added at 2 h postinfection (hpi). Infections were scored by immunoblot analysis or by indirect immunofluorescence microscopy at 30 hpi (HCVcc and SV40), 16 hpi (SeV), or 5 hpi (Sindbis virus).

RNA interference. Subconfluent cultures of PLC/PRF/5 or Huh-7 cells in 6-well plates were transfected twice with 80 pmol of synthetic double-stranded siRNA (Dharmacon) complexed with 4 μl of oligofectamine (Invitrogen) in a total volume of 1 ml of OptiMEM for 6 h. The interval between both siRNA transfections was 48 h. Cells were trypsinized 24 h after the second siRNA transfection and plated in 12-well plates for the HCVpp entry assay, or they were plated in 24-well plates for infection with HCVcc and infected 24 h after trypsinization. Just before infection, extra wells of cells treated with each siRNA were counted to ensure that equal numbers of cells were infected. Relative CHC levels were analyzed by immunoblotting equal amounts of cell lysates. The films were scanned and quantified with the Image J software. The CHC target sequence was UAAUCCAAUUCGAAGACCAAU (34). The control siRNA was originally designed to knock down the green fluorescent protein; its target sequence is GCUGACCCUGAAGUUCAUC.

Indirect immunofluorescence microscopy. Infected cells were processed for immunofluorescent detection of viral proteins as previously described (44). Nuclei were stained by a 1-min incubation in PBS containing 1 μg/ml Hoechst dye 33342. Coverslips were mounted on glass slides using Mowiol and observed with a Zeiss Axiophot equipped with a ×40 magnification, 1.3 numerical aperture oil immersion lens. Fluorescent signals were collected with a Princeton cooled charged device using specific fluorescence excitation and emission filters. Images were processed using Adobe Photoshop software. For quantification, images of 10 randomly picked areas of each coverslip were recorded. Cells labeled with anti-E2 MAb AP33 were counted as infected cells. The total number of cells was obtained from Hoechst-labeled nuclei. The infections were scored as the ratio of infected cells to total cells.

Immunoblotting. Cells were lysed in 50 mM Tris-Cl buffer, pH 7.5, containing 100 mM NaCl, 1 mM EDTA, 1% Triton X-100, 0.1% sodium dodecyl sulfate (SDS), and protease inhibitors, for 30 min on ice. Cells were collected, and the nuclei were pelleted. Protein concentration in the postnuclear supernatants was determined by the bicinchoninic acid method as recommended by the manufacturer (Sigma), using bovine serum albumin as the standard. Five micrograms of total protein was separated by SDS-polyacrylamide gel electrophoresis and transferred to nitrocellulose membranes (Hybond-ECL; Amersham) by using a Trans-Blot apparatus (Bio-Rad). The proteins of interest were revealed with specific primary antibodies followed by donkey anti-goat immunoglobulin G (IgG), goat anti-mouse IgG, or anti-rat IgG conjugated to peroxidase (Jackson Immunoresearch) as well as enhanced chemiluminescence detection (Amersham) as recommended by the manufacturer.

RESULTS

Real-time PCR-based HCVpp entry assay. In order to study HCVpp entry, we first tried to use a luciferase-based assay (37). However, our attempts were quite ineffective, due to drug toxicity and differences in cell proliferation under various experimental conditions, over the 2-day culture period that is necessary for luciferase expression. To overcome these difficulties, we set up a new assay for HCVpp entry, derived from the method originally designed by Mothes et al. for studying retrovirus entry (33). It is based on the quantification by PCR of the cDNA synthesized in target cells during HCVpp entry. In order to quantify early events during HCVpp entry, we designed primers in the U3 region of the LTR, which is the first part of the viral genome to be retrotranscribed during the entry of a retroviral particle (21).

During the development of this assay, we observed that HCVpp infection yielded signals about three times higher in PLC/PRF/5 cells than in Huh-7 cells. This effect was observed with the PCR-based assay as well as with the luciferase-based assay (data not shown). Therefore, most of the experiments were carried out in PLC/PRF/5 cells.

Since HCVpp infection is sensitive to agents that neutralize the pH of endosomes (4, 24), we tested whether we could detect this pH sensitivity with the PCR-based assay in order to confirm that it indeed reflects this entry pathway. The importance of endosome acidification was studied with bafilomycin A1, which is a specific inhibitor of endosomal proton-ATP pumps. PLC/PRF/5 cells were preincubated for 30 min with various concentrations of bafilomycin A1 and infected in the presence of the inhibitor. Results (Fig. 1A) show that the amounts of retroviral DNA recovered from infected cells dramatically decreased for HCVpp and VSV-Gpp in a dose-dependent manner. In contrast, the synthesis of A-MLVpp-derived retroviral DNA was not affected by 20 or 50 nM bafilomycin A1, and it was reduced at 100 nM. Although significant, this reduction was much smaller than that observed for HCVpp and VSV-Gpp at the same concentration. A similar partial inhibition of A-MLVpp infection with 100 nM bafilomycin A1 was previously reported (4). Similar inhibitions of HCVpp and VSV-Gpp infection were observed with Huh-7 cells (data not shown). Inhibition of HCVpp and VSV-Gpp entry, but not of A-MLVpp entry, was also observed in the presence of chloroquine or NH_4Cl in PLC/PRF/5 cells as well as in Huh-7 cells (data not shown). The results obtained with these different inhibitors of endosomal acidification confirmed that the PCR-based entry assay recapitulates HCVpp entry up to the fusion step.

We next examined whether the levels of retroviral DNA synthesis after 3 h of contact predicted the levels of luciferase expression 3 days later. PLC/PRF/5 cells were infected with different dilutions of an HCVpp stock, and they were then either immediately extracted to purify and quantify retroviral DNA or cultured for 3 days and assayed for luciferase activity. Each assay displayed dose dependency, and interassay comparisons revealed a clear correlation between the level of MLV DNA synthesis and the subsequent level of luciferase expression (Fig. 1B). These results indicate that the levels of DNA synthesis at 3 h accurately quantitate the levels of HCVpp entry.

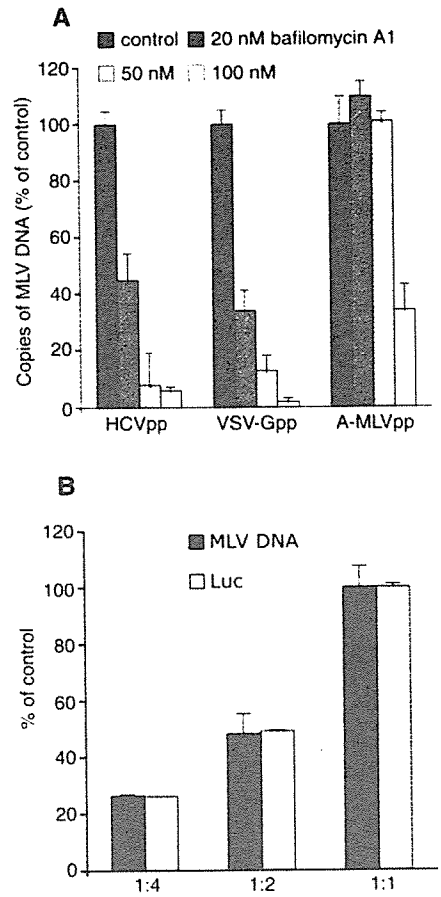

FIG. 1. PCR-based HCVpp entry assay. (A) PLC/PRF/5 cells were pretreated for 30 min with 20, 50, or 100 nM bafilomycin A1 or left untreated. The cells were then infected with HCVpp, VSV-Gpp, or A-MLVpp in the presence of the drug. After 2 h of spinoculation and an additional hour of incubation, total DNA was purified and retroviral DNA was quantified by real-time PCR. Mean values for the controls with no drug were 1.2 equivalent genomes per cell (EG/cell) for HCVpp, 1.5 EG/cell for VSV-Gpp, and 1.3 EG/cell for A-MLVpp infections. The background value obtained from cells infected with pseudotyped particles produced in the absence of envelope proteins corresponded to 0.03 EG/cell. Results were expressed as the percentage of entry in control cells treated with no drug. (B) PLC/PRF/5 cells were infected by spinoculation with different dilutions of the same HCVpp stock. Cells were either immediately lysed to extract DNA or cultured for 3 days to allow for luciferase expression. Retroviral DNA was quantified by real-time PCR (MLV DNA), and infection was quantified by luciferase assay (Luc). Mean values for the undiluted HCVpp infection were 1.3 EG/cell and 6.5×10^6 relative light units (RLU), and the background values obtained from cells infected with pseudotyped particles produced in the absence of envelope proteins corresponded to 0.018 EG/cell and 3.0×10^2 RLU. Results were expressed as the percentage of entry in cells infected with undiluted HCVpp stock (1:1).

HCVpp entry is clathrin dependent. The pH dependency of HCVpp entry implies that HCVpp fusion does not occur at the plasma membrane but from within an intracellular acidic compartment, most probably an endosome. To assess the role of clathrin-mediated endocytosis in HCVpp entry, we first examined the inhibitory effect of chlorpromazine. Chlorpromazine causes clathrin lattice to assemble on endosomal membranes and at the same time prevents the assembly of coated pits at

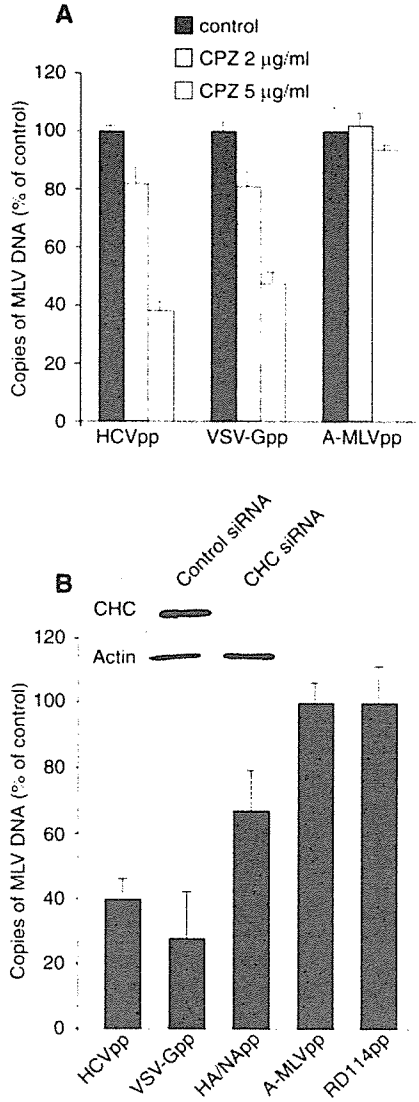

FIG. 2. Clathrin-mediated entry of HCVpp. (A) PLC/PRF/5 cells were pretreated for 30 min with 2 or 5 μg/ml chlorpromazine (CPZ) or were left untreated. The cells were then infected with HCVpp, VSV-Gpp, or A-MLVpp by spinoculation in the presence of the drug. (B) PLC/PRF/5 cells were transfected twice with CHC siRNA or control siRNA, as explained in Materials and Methods. Two days after the second siRNA transfection, cells were spinoculated with HCVpp, VSV-Gpp, HA/NApp, RD114pp, or A-MLVpp. The cellular content of retroviral DNA was quantified by real-time PCR as a measure of entry and is expressed as a percentage of entry in untreated control cells (A) or in cells treated with control siRNA (B). The inset in panel B shows an immunoblot of the relative CHC and actin contents in siRNA-treated cells.

the plasma membrane (57). Chlorpromazine inhibited the entry of HCVpp in PLC/PRF/5 cells in a dose-dependent manner but had minimal effect on A-MLVpp (Fig. 2A). As expected for a clathrin-dependent virus (53), chlorpromazine also inhibited VSV-Gpp entry (Fig. 2A). At 5 μg/ml chlorpromazine, HCVpp entry was inhibited by about 60% and VSV-Gpp entry by about 50%. The use of higher chlorpromazine concentrations resulted in cell detachment during spinoculation of Huh-7 or PLC/PRF/5 cells. This toxicity precluded the use of 10 μg/ml chlorpromazine, a concentration that strongly inhibited bovine viral diarrhea virus infection in MDBK cells (29).

To further confirm that HCVpp entry requires an active pathway of clathrin-mediated endocytosis, we also knocked down the clathrin heavy chain (CHC) using siRNA technology. Following two successive transfections of siRNA, CHC levels were down-regulated to about 20% of controls or less (Fig. 2B). PLC/PRF/5 cells treated with CHC or control siRNA were infected with HCVpp, and entry was quantified by quantitative PCR. For comparison, the entry of retroviral particles pseudotyped with envelope glycoproteins of VSV (VSV-Gpp) or influenza virus (HA/NApp), two viruses known to enter by clathrin-mediated endocytosis, were also quantified. We also monitored the entry of retroviral particles pseudotyped with envelope glycoproteins of two retroviruses known to enter by a nonendocytic route (A-MLVpp and RD114pp). VSV-Gpp entry was strongly inhibited in CHC siRNA-treated cells (Fig. 2B). Similar levels of inhibition were achieved for HCVpp, whereas HA/NApp entry was significantly less inhibited than that of HCVpp and VSV-Gpp, in keeping with the documented dual-entry pathway of influenza virus by both clathrin-mediated and clathrin-independent endocytosis (46, 52). In contrast, the entry of RD114pp or A-MLVpp was not affected by CHC depletion (Fig. 2B), as expected for particles coated with envelope glycoproteins of pH-independent retroviruses. Similar results were obtained with Huh-7 cells (data not shown).

The inhibition of HCVpp entry by chlorpromazine or by CHC depletion strongly suggests that HCVpp enters PLC/PRF/5 cells by clathrin-mediated endocytosis.

HCVcc infection is clathrin dependent. Recently, it has become possible to generate infectious HCV particles in cell culture (HCVcc), allowing the study of HCV entry with infectious viral particles. Preliminary experiments indicated that HCVcc does not infect PLC/PRF/5 cells, in contrast to HCVpp (C. Wychowski, unpublished observation). The reason for this difference is not yet understood, but it may involve a postentry restriction in PLC/PRF/5 cells. Therefore, we used Huh-7 cells to test whether the infection by HCVcc is dependent on clathrin-mediated endocytosis. Huh-7 cells were transfected twice with CHC or control siRNA, infected with HCVcc for 2 h at 37°C, and cultured for 30 h to allow for expression of viral proteins. The cells were then lysed and analyzed by immunoblotting or fixed and processed for immunofluorescence. As shown in Fig. 3A, the expression levels of E2 and NS3 were significantly lower at 30 hpi in CHC siRNA-treated cells than in cells treated with control siRNA or untreated cells. Similar results were obtained at 48 hpi (data not shown).

In comparison, the infection of siRNA-treated Huh-7 cells with Sindbis virus was also monitored. Sindbis virus enters cells by clathrin-mediated endocytosis (6). In order to facilitate the detection of Sindbis virus infection, we used a recombinant Sindbis virus driving the expression of HCV envelope protein E1 in infected cells (16). The infection was detected by immunoblotting cell lysates with anti-E1 (HCV) MAb A4. Note that in these experiments E1 is a transgene that is used as a marker and does not play any role in recombinant Sindbis virus entry. As expected, CHC depletion also had an inhibitory effect on Sindbis virus infection (Fig. 3A).

As a control, we infected siRNA-treated cells with SV40,

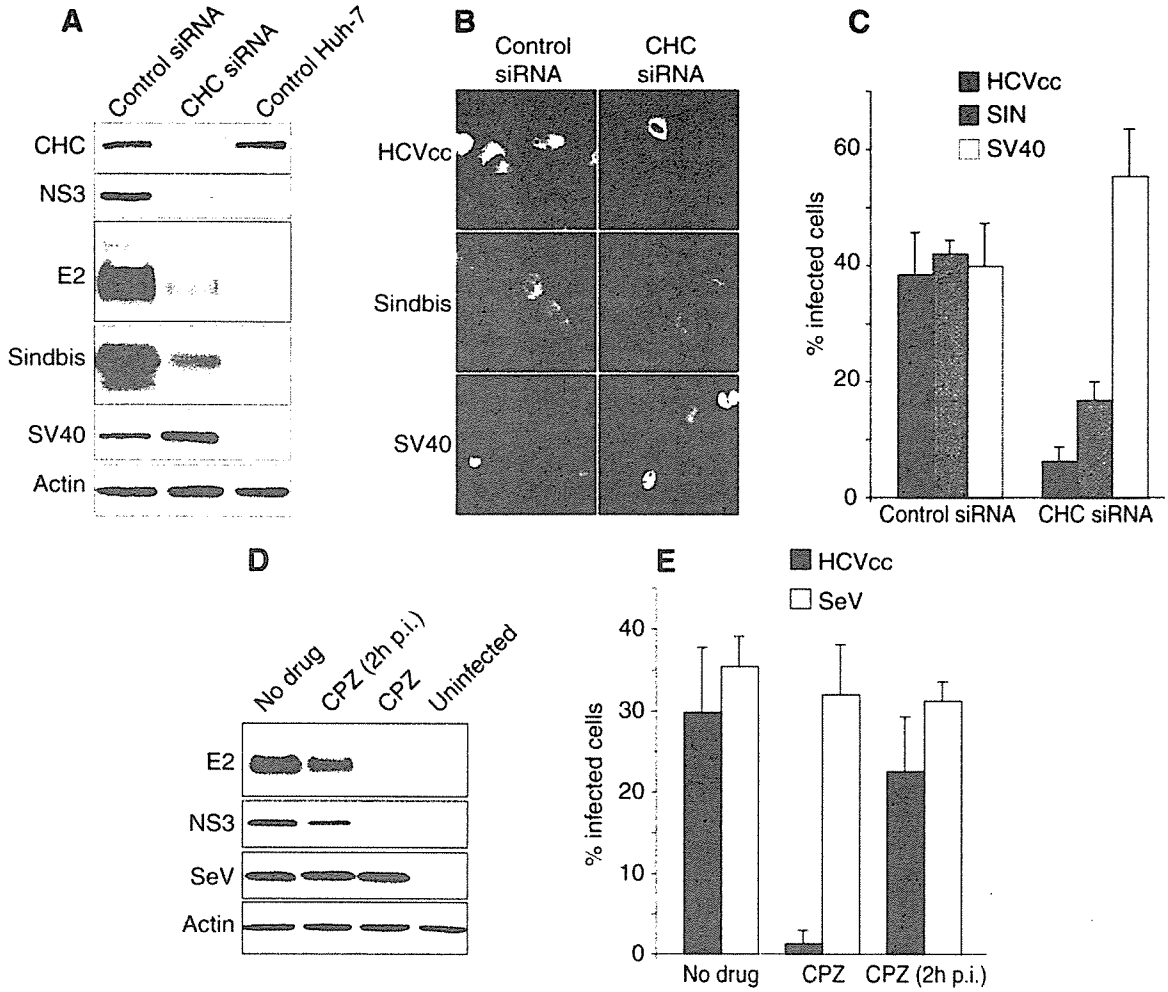

FIG. 3. Clathrin-mediated entry of HCVcc. (A to C) Huh-7 cells were treated with CHC or control siRNA and then infected with HCVcc, a recombinant Sindbis virus expressing HCV E1, or SV40. (A) Cells were lysed at 5 hpi (Sindbis) or 30 hpi (HCVcc and SV40), and the cell lysates were analyzed by immunoblotting with antibodies to E2, NS3 (HCVcc), E1 (Sindbis), T-antigen (SV40), CHC, and actin. (B) Cells were fixed and processed for immunofluorescent detection of E2 (HCVcc), E1 (Sindbis), or T antigen (SV40). (B) For each virus, the fields presented contain similar numbers of CHC or control siRNA-treated cells. (C) Percentage of infected cells in CHC and control siRNA-treated cells. (D and E) Huh-7 cells were pretreated for 30 min and then infected for 2 h with HCVcc in the presence or the absence of chlorpromazine (CPZ; 5 μg/ml). Cells infected in the absence of drug were cultured with no drug, or chlorpromazine was added 2 hpi (CPZ 2hpi). Infection was analyzed (D) by immunoblotting with antibodies to E2, NS3, GFP (SeV), and actin or (E) by immunofluorescent detection of infected cells using an anti-E2 MAb (HCVcc) or by GFP fluorescence (SeV). Results are presented as percentages of infected cells.

which enters by clathrin-independent endocytosis in Huh-7 cells (12). Cells were lysed at 30 hpi, and the levels of T antigen were visualized by immunoblotting. In contrast to HCV and Sindbis virus, SV40 infection was not inhibited in CHC-depleted cells. Instead, we consistently observed in cells treated with CHC siRNA higher levels of T-antigen expression than in cells treated with control siRNA (Fig. 3A). Similar results were obtained with other unrelated control siRNAs (data not shown), thus excluding an inhibitory effect of the control siRNA on SV40 infection or T-antigen expression. This apparent up-regulation of SV40 infection upon CHC depletion was not further investigated in this study.

To verify that the lower levels of HCV proteins observed by immunoblotting resulted from an inhibition of the infection and not from a reduced expression of HCV proteins, infected cells were analyzed by immunofluorescence microscopy. The expression levels of HCV, Sindbis virus, or SV40 proteins in individual cells appeared similar in CHC siRNA-treated cells and in controls (Fig. 3B and data not shown). The number of cells infected by HCVcc was reduced in CHC siRNA-treated cells by about 80% (Fig. 3C). Similar results were obtained when HCVcc infection was scored with an anti-C MAb (data not shown). The number of Sindbis virus-infected cells was also reduced in CHC siRNA-treated cells (by 60%), whereas SV40-infected cells were present in increased numbers (Fig. 3C). These data confirmed the inhibitory role of CHC depletion on HCVcc infection.

The role of clathrin-mediated endocytosis in HCV infection was further confirmed with chlorpromazine. When Huh-7 cells were pretreated with chlorpromazine for 30 min and then infected with HCVcc, the expression levels of E2 and NS3 were dramatically reduced (Fig. 3D) and the number of infected

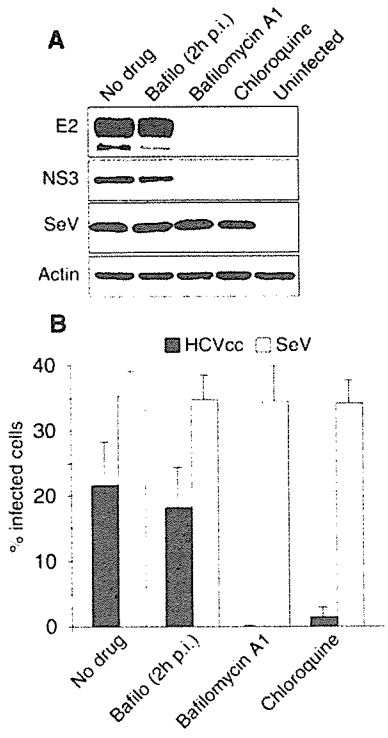

FIG. 4. pH dependency of HCVcc infection. Huh-7 cells were pretreated for 30 min and then infected with HCVcc or SeV in the presence of 50 nM bafilomycin A1 or 20 μM chloroquine or in the absence of any inhibitor of endosomal acidification. Cells infected in the absence of drug were cultured with no drug, or bafilomycin A1 was added 2 hpi (Bafilo 2hpi). HCVcc infection was analyzed (A) by immunoblotting with antibodies to E2, NS3, GFP (SeV) and actin or (B) by immunofluorescent detection of infected cells using an anti-E2 MAb (HCVcc) or by GFP fluorescence (SeV). Results are presented as percentages of infected cells.

cells was very low (Fig. 3E). In contrast, when Huh-7 cells were infected in the absence of chlorpromazine and the drug was added 2 hpi, the expression levels of HCV proteins E2 and NS3 were only slightly reduced (Fig. 3D), and the number of infected cells was similar to that in control untreated cells (Fig. 3E).

As a control, we assessed the impact of chlorpromazine on the infection of Huh-7 cells by Sendai virus (SeV). SeV is a paramyxovirus which enters by direct fusion at the plasma membrane. To facilitate detection, we used a recombinant SeV expressing GFP (28). Chlorpromazine treatment had no effect on the levels of GFP expression (Fig. 3D) or the number of SeV-infected cells (Fig. 3E). These results indicate that the inhibitory effect of chlorpromazine on HCVcc infection primarily results from an inhibition of an early step of the infection, most probably corresponding to entry.

Taken together, the data obtained with CHC depletion and chlorpromazine treatment indicate that HCVcc entry is dependent on an active pathway of clathrin-mediated endocytosis.

HCVcc infection is pH dependent. Since both HCVpp entry and HCVcc infection assays indicated a functional role for clathrin-mediated endocytosis in HCV entry, we also verified that HCVcc infection is indeed dependent on acidic endosomal pH. Huh-7 cells were pretreated for 30 min, infected for 2 h with HCVcc, and cultured for 30 h in the presence of 50 nM bafilomycin A1 or 20 μM chloroquine. These experimental conditions were chosen because they had a strong inhibitory effect on HCVpp entry in PLC/PRF/5 cells and on BVDV infection in MDBK cells (29). HCVcc infection was quantified by immunoblotting. As shown in Fig. 4A, the cellular levels of both E2 and NS3 at 30 hpi were dramatically reduced in the presence of each inhibitor compared to levels for untreated control cells infected with the same amounts of HCVcc. When the cells were infected and bafilomycin A1 was added to infected cells at 2 hpi, the levels of E2 and NS3 were similar to those in the controls, indicating that the drug had no inhibitory effect on HCVcc infection at a postentry step. In contrast, bafilomycin A1 and chloroquine had no effect on the levels of GFP expression mediated by recombinant SeV infection (Fig. 4A).

HCVcc infection was also scored by immunofluorescence microscopy using anti-E2 and anti-C antibodies. No infected cells were observed in cells pretreated and infected in the presence of 50 nM bafilomycin A1 (Fig. 4B and data not shown). In contrast, cells that were infected with no drug and incubated with 50 nM bafilomycin A1 from 2 hpi up to 30 hpi displayed a percentage of infected cells similar to that of controls. Chloroquine also dramatically reduced the number of infected cells (Fig. 4B). In contrast, neither bafilomycin A1 nor chloroquine treatments had any impact on the number of SeV-infected cells (Fig. 4B).

Together with the results from immunoblot analysis, these results indicate the HCVcc entry is sensitive to agents that neutralize the acidic pH of cellular endosomes.

DISCUSSION

To examine the entry of HCV in target cells, we have used two complementary approaches. First we have developed a new assay based on the use of HCVpp to specifically study early entry steps mediated by HCV envelope glycoproteins. This assay is based on the quantification of retroviral DNA synthesis, which occurs soon after the fusion of the retroviral particle with a cellular membrane (21). Presumably, this assay is only dependent on the entry steps mediated by the heterodimer E1E2 (binding, endocytosis, and fusion) and on the activity of the reverse transcriptase of the HCVpp retroviral core. Second, we made use of the recently developed JFH-1 infectious clone to investigate in parallel the entry pathway of HCVcc in the context of an infectious cycle.

Both assays yielded similar conclusions on the mechanisms of HCV entry. Our results indicate that HCVpp and HCVcc enter cells by clathrin-mediated endocytosis. The partial inhibition observed in cells transfected with CHC siRNA is probably due to the incomplete depletion of clathrin from the cells after siRNA treatment rather than to the existence of an alternative entry pathway for HCV, since a similar behavior was observed for Sindbis virus and VSV-Gpp, two controls for clathrin-mediated viral entry (6, 53). HCVcc infection was also found to be sensitive to agents that interfere with the acidic pH of endosomes. Similar findings on the pH dependency of HCVcc entry were recently reported by Tscherne et al. with a recombinant HCVcc clone expressing luciferase (54). This is consistent with an entry mediated by clathrin-mediated endocytosis, since clathrin-coated vesicles deliver their content into endosomes with an acidic content.

Many other viruses are known to hijack endocytic pathways. The sensitivity to lysosomotropic agents has often been considered evidence for an entry by endocytosis. However, viruses insensitive to lysosomotropic agents may also enter cells by endocytosis (12, 20, 33, 40). Several endocytic pathways were recently identified in addition to the clathrin-mediated pathway (10, 39, 51). These newly discovered pathways differ in the type of vesicular carrier formed at the plasma membrane to carry out the internalization step and also differ in the type of intracellular compartments to which the internalized material is transported. Some of them carry ligands to the classical acidic early and late endosomes, which are also reached by endocytic ligands originating from clathrin-coated vesicles, while other ones deliver their ligands to compartments with neutral pH, such as caveosomes, endoplasmic reticulum, or the Golgi complex (35, 39). Not surprisingly, it appears that viruses have evolved to adapt to these different entry routes. Several enveloped and nonenveloped viruses have been reported to use various alternative endocytic pathways, whether they are sensitive or not to acidic pH. SV40 enters through caveola-mediated internalization in CV-1 cells (40). Echovirus 1 and rotavirus are internalized by clathrin- and caveola-independent pathways, which require dynamin function and are sensitive to the cholesterol-sequestering drug methyl-β-cyclodextrin (41, 47). Lymphocytic choriomeningitis virus is endocytosed into cells by noncoated vesicles and reaches an acidic intracellular compartment where a process of pH-dependent fusion occurs (5). Influenza viruses can be endocytosed both by clathrin-independent and clathrin-dependent mechanisms into the same cell (46, 52).

During experiments involving CHC depletion, we made use of SV40 as a control for clathrin-independent endocytosis. SV40 was recently reported to infect Huh-7 cells by a unique route involving neither clathrin-mediated endocytosis nor the internalization of caveolae, which are absent from Huh-7 cells (12). In Huh-7 cells, the endocytosis of SV40 virions occurs through small uncoated vesicles that are formed at the plasma membrane in a dynamin-independent manner, and they are sensitive to cholesterol-sequestering drugs (12). Interestingly, we found that the depletion of clathrin heavy chain results in an increased SV40 infection, possibly by enhancing its endocytic pathway. It is well established that many regulatory factors have opposite effects on clathrin-mediated and on caveolae/lipid raft-mediated endocytosis (38). We can therefore hypothesize that the inhibition of clathrin-mediated endocytosis might induce compensatory mechanisms up-regulating alternative endocytic pathways in order to control the homoeostasis of the plasma membrane. Similarly, up-regulation of dynamin-independent fluid-phase uptake has been reported in cells expressing dominant-negative dynamin mutants (11).

In the *Flaviviridae* family, the entry of viruses of the *Flavivirus* and *Pestivirus* genera was examined before. Early electron microscopy studies suggested that the flavivirus West Nile virus enters cells through clathrin-coated vesicles (22). This mode of entry was recently confirmed by the use of a dominant-negative form of Eps15 as a way to functionally probe the clathrin-mediated pathway (8). This is consistent with numerous studies which have shown that the envelope glycoprotein E of flaviviruses undergoes a conformational transition under acidic conditions from a native dimeric form to a fusogenic trimeric form (23). Such an acid-triggered conformational transition has not been reported at the present time for the envelope proteins of pestiviruses or HCV.

The pestivirus BVDV also enters by clathrin-mediated endocytosis (26, 29). Consistent with this mode of entry, BVDV infection is sensitive to agents that neutralize the pH of endosomes. However, unlike flaviviruses, BVDV and HCVcc particles are stable and stay infectious when incubated at acidic pH before infection (26, 54). In similar conditions, flaviviruses, alphaviruses, and other enveloped viruses are inactivated, presumably because the pH triggers irreversible conformational changes in the envelope glycoproteins of these viruses similar to those associated with the fusion process during entry. This indicates that a pH drop is not sufficient to induce the conformational changes associated with the fusion process mediated by the envelope glycoproteins of pestiviruses and hepaciviruses, or that the changes in conformation triggered under acidic conditions are reversible in the absence of a cellular membrane. Such reversible conformational changes were reported for VSV (43).

It has been suggested that HCV and BVDV envelope glycoproteins must be primed to acquire a fusogenic conformation triggered by pH. This priming event can be mimicked to some extent by pretreating BVDV particles with reducing agents (26). Under reducing conditions, BVDV virions became pH sensitive, and their fusion to the plasma membrane was inducible at pH 5.

Our study suggests that, like flaviviruses and pestiviruses, HCV enters cells through clathrin-mediated endocytosis and fusion from within an acidic endosomal compartment. At the present time, we still do not know the exact nature of the endosomal compartment that is competent for HCV fusion. We also do not know whether the acidic pH of endosomes acts directly on the conformation of HCV envelope glycoproteins E1 and E2 to trigger fusion or whether it acts indirectly by activating other endosomal agents, which in turn would promote HCV fusion. It would be interesting to determine if HCV fusion requires a priming event to allow an acid-triggered conformational change of the E1E2 heterodimer or if the fusion may be directly induced by a pH drop, as is the case for flaviviruses. Tscherne et al. recently reported that HCVcc infection by direct fusion at the plasma membrane induced by a pH drop was very inefficient (54). However, it is not known if the blockade was at the fusion step or at a postfusion step. On the other hand, experiments carried out in vitro with HCVpp indicated that fusion to liposomes mediated by HCV E1E2 heterodimer is readily inducible at acidic pH (27). This suggests that a preliminary priming event would not be necessary for HCV E1E2-mediated fusion. It remains to be determined if conformational changes in E1E2 are associated with the fusion process and if similar findings are observed with HCVcc particles. Such questions could be addressed once it becomes possible to purify HCVcc particles for in vitro studies.

ACKNOWLEDGMENTS

We thank Laetitia Corset and Anne Goffard for help with real-time PCR. We are grateful to J. F. Delagneau, A. Patel, and J. McKeating for providing us with antibodies, D. Lavillette and F.-L. Cosset for plasmids, and L. Roux and F. Lafont for the purified stock of SeV. Some data were generated with the help of the Imaging Core Facility of the Calmette campus.